

Polynomial-Time Preparation of Low-Temperature Gibbs States for 2D Toric Code

Zhiyan Ding^{*1}, Bowen Li^{†2}, Lin Lin^{‡1,3}, and Ruizhe Zhang^{§4}

¹Department of Mathematics, University of California, Berkeley

²Department of Mathematics, City University of Hong Kong

³Applied Mathematics and Computational Research Division, Lawrence Berkeley National Laboratory

⁴Simons Institute for the Theory of Computing

Abstract

We propose a polynomial-time algorithm for preparing the Gibbs state of the two-dimensional toric code Hamiltonian at any temperature, starting from any initial condition, significantly improving upon prior estimates that suggested exponential scaling with inverse temperature. Our approach combines the Lindblad dynamics using a local Davies generator with simple global jump operators to enable efficient transitions between logical sectors. We also prove that the Lindblad dynamics with a digitally implemented low temperature local Davies generator is able to efficiently drive the quantum state towards the ground state manifold. Despite this progress, we explain why protecting quantum information in the 2D toric code with passive dynamics remains challenging.

1 Introduction

The ability (or the lack of it) to efficiently prepare Gibbs states has far-reaching implications in quantum information theory, condensed matter physics, quantum chemistry, statistical mechanics, and optimization. Given a quantum Hamiltonian $H \in \mathbb{C}^{2^N \times 2^N}$, we would like to prepare the associated thermal state $\sigma_\beta \propto e^{-\beta H}$, where β is the inverse temperature. A number of quantum algorithms have been designed to efficiently prepare high-temperature Gibbs states with a small $\beta = \mathcal{O}(\text{poly}(N^{-1}))$ [PW09, CS17, VAGGdW17, GSLW19, ACL23]. However, as the temperature lowers (i.e., β becomes large), the complexity of these algorithms can scale exponentially in the number of qubits N , rendering them impractical for low-temperature regimes where the Gibbs state has a significant overlap with the ground state of H .

Recent advancements have rekindled interest in designing quantum Gibbs samplers based on Lindblad dynamics [ML20, RWW23, CB21, CKBG23, CKG23, WT23, DLL24]. These

^{*}zding.m@berkeley.edu.

[†]bowen.li@cityu.edu.hk.

[‡]linlin@math.berkeley.edu.

[§]rz Zhang@berkeley.edu.

algorithms rely on a specific form of open quantum system dynamics to drive the system toward its thermal equilibrium, an idea pioneered by Davies in the 1970s [Dav70, Dav74]. The efficiency of such algorithms largely depends on the mixing time of the underlying dynamics, which can vary significantly across different systems and different forms of Lindbladians.

The computational complexity of preparing quantum Gibbs states, computing partition functions, and the potential for establishing quantum advantage in these tasks is a topic of ongoing debate in the literature. On one hand, at high enough temperatures, there exists polynomial-time classical algorithms to sample from Gibbs states and to estimate partition functions [BCGW21, MH21, YL23, BLMT24]. On the other hand, in the low-temperature regime, preparing classical Gibbs states is already NP-hard in the worst case [Bar82, Sly10], and we do not expect efficient quantum algorithms in these cases. The development of these new Gibbs samplers has also contributed to advancements in our complexity-theoretic understanding [RFA24, BCL24, RW24]. [RFA24] proved that simulating the Lindbladian proposed in [CKG23] to time $T = \text{poly}(N)$ at $\beta = \Omega(\log(N))$ for a k -local Hamiltonian is BQP-complete. [BCL24, RW24] constructed a family of k -local Hamiltonians such that quantum Gibbs sampling at constant temperatures (lower than the classically simulatable threshold) can be efficiently achieved with the block-encoding framework [CKBG23], and the task is classically intractable assuming no collapse of the polynomial hierarchy.

None of these constructions imply efficient preparation of Gibbs states at low temperatures. Indeed, when the temperature is sufficiently low, the Gibbs state can exhibit a high overlap with the ground state, and cooling to these temperatures is expected to be QMA-hard in the worst case. However, it is important to recognize that QMA-hardness does not preclude the possibility of developing efficient Gibbs samplers for *specific* Hamiltonians. Consequently, understanding and controlling the mixing time for specific systems (or specific classes of systems) is a fundamental open question in this field and can provide valuable insights into the practical performance of these Gibbs samplers [AFH09, TK15, Tem17, FHGW14, BLP⁺16, Fre18, TKR⁺10, KT13, KB16, BCG⁺23, KACR24, BCG⁺24, RFA24].

In this work, we propose a novel Gibbs sampler with nonlocal jump operators, and analyze its convergence rate for preparing *low-temperature* Gibbs states of the 2D toric code [Kit03], a paradigmatic model in quantum information theory, quantum error correction, and condensed matter physics. In the context of thermalization, when the toric code is exposed to thermal noise modeled by a specific form of Lindbladians called the Davies generator, the seminal work of Alicki et al. [AFH09] showed that the inverse spectral gap (which leads to an upper bound of the mixing time) grows exponentially with inverse temperature β . Using a different argument based on energy barriers, Temme et al. [TK15, Tem17] confirmed that the thermalization time (i.e., mixing time of the Lindblad dynamics) of the 2D toric code with local noise should indeed scale exponentially with β . However, it is unknown whether the $\exp(\beta)$ factor in the mixing time is unavoidable for *all* Lindblad dynamics on this problem. This leads to the central question of this work:

Can we design a quantum algorithm, based on Lindblad dynamics, that efficiently prepares the low-temperature Gibbs state of the 2D toric code with a polynomial runtime in both the inverse temperature β and the number of qubits N ?

Notations. For a finite-dimensional Hilbert space \mathcal{H} , we denote by $\mathcal{B}(\mathcal{H})$ the space of bounded operators with identity element $\mathbf{1}$. We let $\mathcal{D}(\mathcal{H}) := \{\rho \in \mathcal{B}(\mathcal{H}) ; \rho \geq 0, \text{Tr}(\rho) = 1\}$

be the set of quantum states. Denoting by X^\dagger the adjoint operator of $X \in \mathcal{B}(\mathcal{H})$, we recall the Hilbert–Schmidt (HS) inner product on $\mathcal{B}(\mathcal{H})$: $\langle X, Y \rangle := \text{Tr}(X^\dagger Y)$. With some abuse of notation, the adjoint of a superoperator $\Phi : \mathcal{B}(\mathcal{H}) \rightarrow \mathcal{B}(\mathcal{H})$ for $\langle \cdot, \cdot \rangle$ is also denoted by Φ^\dagger . Moreover, $\{X, Y\} = XY + YX$ and $[X, Y] = XY - YX$ for $X, Y \in \mathcal{B}(\mathcal{H})$ denote the anti-commutator and commutator, respectively. We will use the standard asymptotic notations: \mathcal{O} , Ω , and Θ . Precisely, we write $f = \Omega(g)$ if $g = \mathcal{O}(f)$, and $f = \Theta(g)$ if $f = \mathcal{O}(g)$ and $g = \mathcal{O}(f)$.

1.1 Contribution

We derive a perhaps counterintuitive result regarding the 2D toric code: by employing a Lindbladian composed of a local Davies generator supplemented with simple global jump operators that facilitate transitions between logical sectors to overcome the energy barrier, it is possible to efficiently prepare the Gibbs state of the 2D toric code at any temperature. Furthermore, ignoring the information in the logical space, the local Davies generator alone suffices to efficiently drive the density matrix towards the ground state manifold in the zero temperature limit. This approach circumvents the previously established exponential dependence of the mixing time on β , achieving a polynomial scaling with system size (the number of qubits N).

To be specific, given $\beta > 0$, we construct the following Davies generator:

$$\mathcal{L}_\beta = \underbrace{\sum_{j=1}^N \mathcal{L}_{\sigma_j^x} + \mathcal{L}_{\sigma_j^y} + \mathcal{L}_{\sigma_j^z}}_{:= \mathcal{L}_{\text{local full}}} + \underbrace{\mathcal{L}_{X_1} + \mathcal{L}_{Z_1} + \mathcal{L}_{X_2} + \mathcal{L}_{Z_2}}_{:= \mathcal{L}_{\text{global}}}, \quad (1.1)$$

where $\mathcal{L}_{[\cdot]}$ is the standard Davies generator defined via Eq. (2.4) based on 2D toric code Hamiltonian (4.1), and X_1, Z_1, X_2, Z_2 are global logic operators for 2D toric code, see Eq. (4.4) in Section 4. Then, we prove the following main results:

Theorem 1 (Fast mixing of 2D toric code). *The spectral gap of the Gibbs sampler \mathcal{L}_β in (1.1) has the following lower bound*

$$\text{Gap}(-\mathcal{L}_\beta) = \max \left\{ e^{-\mathcal{O}(\beta)}, \Omega(N^{-3}) \right\}.$$

Our proof is valid for all temperatures, which includes two important regimes: 1. finite temperature regime $\beta = \mathcal{O}(1)$; 2. low temperature regime $\beta \gg 1$. In the first case of $\beta = \mathcal{O}(1)$, the local Davies generator $\mathcal{L}_{\text{local full}}$ is sufficient to ensure the spectral gap of \mathcal{L}_β at least $\exp(-\Theta(\beta))$ and independent of N . This is consistent with the result in [AFH09, Theorem 2]. In the second case of $\beta \gg 1$, the Davies generator with global jumps $\mathcal{L}_{\text{global}}$ significantly increases the spectral gap of \mathcal{L}_β , achieving a lower bound of order $\text{poly}(N^{-1})$ and independent of β .

The choice of the global jump operators in (1.1) is natural. As $\beta \rightarrow \infty$, the thermal state converges toward the ground state of the Hamiltonian. Since the 2D toric code has four degenerate ground states that are not locally connected, the local Davies generator $\mathcal{L}_{\text{local full}}$ cannot efficiently transit between these ground states, resulting in a slow mixing process. To overcome this difficulty, we introduce the global jump operators $\mathcal{L}_{\text{global}}$ that

enable transitions between different ground states at low temperatures, which ensures fast mixing even at zero temperature. This phenomenon is not unique to the 2D toric code. For example, in our paper, we also consider a simpler 1D Ising model in Appendix A, construct a similar Davies generator with global jump operators, and demonstrate a fast mixing result similar to Theorem 1 to illustrate the proof concept.

Our proof implies a more detailed characterization of the mixing process. The algebra of observables for 2D toric code can be expressed as a tensor product between a logical observable space and a syndrome space. The spectral gap of the Lindbladian in the logical space and the syndrome space can be analyzed independently. We find that for the standard Davies generator with only local jump operators, the exponentially vanishing spectral gap on β is *only* due to the action on the logical space, where the 2D toric code has four linearly independent ground states that are not locally connected. On the other hand, we show that the spectral gap of the local Davies generator, when restricted to the syndrome space (by tracing out the logical subspace), has a lower bound that decays polynomially with the size of the system and remains independent of β in the low-temperature regime. This is summarized in the following proposition:

Proposition 2. *Let $\mathcal{L}_{\text{local full}}$ be defined as in Eq. (1.1). Then a part of $\mathcal{L}_{\text{local full}}$ admits the syndrome subspace as an invariant subspace and exhibits a “large” spectral gap.*

Specifically, there is a subset of Paulis $\{p_i\} \subset \{\sigma_j^{x/y/z}\}$, which defines $\mathcal{L}_{\text{local}} = \sum_i \mathcal{L}_{p_i}$, a decomposition $\mathcal{H} = \mathbb{C}^{2^N} = \mathcal{H}_{\text{logic}} \otimes \mathcal{H}_{\text{syndrome}}$ with $\mathcal{H}_{\text{logic}} \cong \mathbb{C}^4$ and $\mathcal{H}_{\text{syndrome}} \cong \mathbb{C}^{2^{N-2}}$, and a corresponding decomposition $\mathcal{B}(\mathcal{H}) \cong \mathcal{B}(\mathcal{H}_{\text{logic}}) \otimes \mathcal{B}(\mathcal{H}_{\text{syndrome}})$, such that

$$\mathcal{L}_{\text{local}}(\mathcal{B}(\mathcal{H}_{\text{logic}}) \otimes \mathcal{B}(\mathcal{H}_{\text{syndrome}})) = \mathcal{B}(\mathcal{H}_{\text{logic}}) \otimes \mathcal{L}_{\text{local}}(\mathcal{B}(\mathcal{H}_{\text{syndrome}})) .$$

The spectral gap of $-\mathcal{L}_{\text{local}}$ restricted to the syndrome space $\mathcal{B}(\mathcal{H}_{\text{syndrome}})$ is lower bounded by

$$\max \{ \exp(-\mathcal{O}(\beta)), \Omega(N^{-3}) \} .$$

The above proposition implies that, even in the absence of the global jump operator, the system thermalizes quickly within the syndrome space. This is a key step towards proving Theorem 1; see Section 3 for further details. Here the operator $\mathcal{L}_{\text{local}}$ in Proposition 2 is carefully designed so that analyzing syndrome mixing reduces to studying the spectral gap of two distinct Glauber dynamics with quasi-1D classical Ising Hamiltonians (precisely, on the “snake” and “comb”, see Fig. 3) at low temperature. We then introduce a new iterative method to establish lower bounds of their spectral gaps. To the best of our knowledge, this result concerning low-temperature thermalization for such quasi-1D classical Ising models is also novel in the literature.

1.2 Implications

Mixing time for preparing low-temperature Gibbs state. In this paper, we mainly focus on estimating the spectral gap of the Lindblad generator. It is well known that a lower bound on the spectral gap provides an upper bound on the mixing time of the Lindblad dynamics [TKR⁺10]. Specifically, for a detailed balanced Lindblad generator \mathcal{L} with a spectral gap lower bounded by α and the unique fixed point σ_β , the following holds:

$$\|e^{t\mathcal{L}^\dagger} \rho - \sigma_\beta\|_{\text{tr}}^2 \leq \chi^2(e^{t\mathcal{L}^\dagger} \rho, \sigma_\beta) \leq \chi^2(\rho, \sigma_\beta) e^{-2\alpha t} ,$$

where $\chi^2(\rho, \sigma_\beta) = \text{Tr}[(\rho - \sigma_\beta)\sigma_\beta^{-1/2}(\rho - \sigma_\beta)\sigma_\beta^{-1/2}]$ is the χ^2 -divergence. Notice that

$$\max_{\rho} \chi^2(\rho, \sigma_\beta) \leq (\lambda_{\min}(\sigma_\beta))^{-1} \leq 2^N e^{\beta \|H\|},$$

with $\lambda_{\min}(\cdot)$ denoting the minimal eigenvalue. For 2D toric code Hamiltonian, we have the operator norm $\|H\| = \mathcal{O}(N)$. Thus, it readily gives an upper bound of the mixing time $t_{\text{mix}}(\epsilon) := \{t \geq 0; \|e^{t\mathcal{L}^\dagger} \rho - \sigma_\beta\|_{\text{tr}} \leq \epsilon, \forall \text{ quantum states } \rho\}$ for a fixed ϵ :

$$t_{\text{mix}}(\epsilon) = \mathcal{O}\left(\frac{1}{\alpha} (N + \beta)\right).$$

By substituting the spectral gap estimate from Theorem 1, the mixing time of \mathcal{L}_β in Eq. (1.1) scales as $\mathcal{O}(\min\{\beta \text{poly}(N), \exp(c\beta)(N + \beta)\})$ for some universal constant c , which is a significant improvement over the $\mathcal{O}(\exp(c\beta)(N + \beta))$ bound given in [AFH09] when $\beta \gg 1$. It is worth mentioning that in both cases, the mixing time scales polynomially with the number of qubits, N , which is referred to as *fast mixing* in the literature. In our case, the N dependence arises from both the spectral gap and the prefactor $\max_{\rho} \chi^2(\rho, \sigma_\beta)$. While the latter dependence can sometimes be improved to $\mathcal{O}(\log(N))$ by considering the relative entropy distance [BCG⁺23, BCG⁺24, KACR24], achieving the *rapid mixing* regime. This would also require translating the spectral gap lower bound into a constant or $\Omega(\log(N)^{-1})$ lower bound for the modified logarithmic Sobolev inequality (MLSI) constant. This presents an interesting direction for future exploration.

Thermal state versus ground state preparation: The 2D toric code is a stabilizer Hamiltonian, and its ground state can be efficiently prepared by measuring all stabilizers. The ground state can also be prepared using carefully designed dissipative state engineering approaches (see e.g. [VWC09]). However, these approaches do not easily generalize to algorithms for thermal state preparation. The fast mixing result at low temperatures in this work suggests that thermal state preparation methods can also serve as a generic tool for approximate ground state preparation by selecting a sufficiently low temperature. Specifically, as discussed in Proposition 2, the local Davies generator within the syndrome space has a spectral gap that decays only polynomially with system size as β approaches infinity. This implies that at fixed sufficiently low temperature ($\beta \gg 1$), once a quasi-particle pair (an elementary excited state of the 2D toric code, see Section 4.1) appears in the system, the local Davies generator can eliminate it in $\mathcal{O}(\text{poly}(N))$ time. Consequently, if the goal is to efficiently prepare *some* ground state while discarding logical information, it is sufficient to use local Davies generators, and the time required is much shorter than that for equilibrating all logical sectors using local Davies generators. This result may be of independent interest, as nature itself often prepares ground states by cooling.

Fast thermalization from a ground state: A natural question regarding the thermalization of the toric code Hamiltonian is: if one starts from the ground state, doesn't it take exponential time in β to create even one quasi-particle pair in the first place? While this is correct, and may seem paradoxical, it does not contradict our main result that the thermalization time scales polynomially in β . The reason is that although creating one quasi-particle

pair from the ground state takes an exponential amount of time in β to create one quasi-particle pair from the ground state, the fraction of the excited state in the thermal state is exponentially small in β . In the case of 2D toric code, the slow thermalization of local Davies generators at low temperatures mainly stems from the need to achieve an equal population across all ground states. In other words, the challenge of thermalization lies mainly in transitioning between orthogonal ground states, as discussed in Section 1.1. In our work, we prove that spectral gap of the global jump operators restricted to the logical space is, independent of β at low temperatures. This allows the system to equilibrate rapidly, even starting from a ground state.

Fast thermal state preparation versus quantum memory: A good *self correcting quantum memory* (SCQM) should be able to store a quantum state in contact with a cool thermal bath for a duration that increases exponentially with the size of the system. If the thermalization time of a quantum system only scales polynomially with system size, it cannot be considered a viable candidate for SCQM. Ref. [AFH09] demonstrated that, at any constant temperature, the 2D toric code has a spectral gap that remains independent of system size, and thus is not a good SCQM, and to date valid candidates for SCQM are only known in 4D or higher [AHHH10]. Our refined estimate indicates that local Davies generator at low temperature (or even at zero temperature) can be efficient in annihilating quasi-particles in the syndrome space.

A natural question is: does it make the 2D toric code a candidate for *passively protected quantum memories* (sometimes known as autonomous quantum error correction, autonomous quantum memory protection) [BW00, LKV⁺13, LLG24]? Specifically, consider a Lindbladian $\mathcal{L} = \mathcal{L}_e + \mathcal{L}_r$ where \mathcal{L}_e is a Davies generator modeling thermal noise at some finite temperature β^{-1} , and \mathcal{L}_r is a Davies generator at near-zero temperature (implemented either digitally or using analogue devices), and the number of terms (each of up to unit strength) in \mathcal{L}_r can scale polynomially in N . Starting from a pure ground state ρ_0 carrying well-defined logical information, we run the dynamics for some fixed time t , and then apply a single round of decoding map \mathcal{E}_d to obtain a final density matrix ρ_f . Can we ensure that the trace distance between ρ_0 and ρ_f decreases super-polynomially in N ? Unfortunately, the answer is very likely negative for the 2D toric code. The reason is that once \mathcal{L}_e creates a syndrome in the form of a quasi-particle excitation, this quasi-particle can be diffused by either \mathcal{L}_e or \mathcal{L}_r at zero energy cost. As a result, in the worst case, a quasi-particle may diffuse across the torus in polynomial time before it is annihilated, which changes the logical information. In this sense, the key difference between protecting logical information through passive dynamics and using quantum error correction is that the latter actively guides the diffusion and annihilation of quasi-particles in a way that preserves the logical information.

Notably, this problem does not arise in 2D Ising models for which local excitations cannot diffuse without incurring an energy cost. This is a key aspect in recent designs of passively protected quantum memories [LLG24]. To our knowledge, the theoretical analysis of such models remains an open question.

1.3 Related works

The thermalization of stabilizer Hamiltonians using a local Davies generator has been explored in several prior works [AFH09, TK15, Tem17, FHGW14, BLP⁺16, Fre18]. In [AFH09],

the authors demonstrated that the local Davies generator achieves fast thermalization for the 2D toric code. In particular, the spectral gap of the Davies generator, when considering all local Pauli coupling operators, is lower bounded by $\exp(-\Theta(\beta))$. The bound is valid for all temperatures and results in a mixing time (defined via the trace distance) scaling as $t_{\text{mix}} = N \exp(\Theta(\beta))$. Along the same direction, [TK15, Tem17] considered general stabilizer codes and establish a lower bound on the spectral gap (or Poincaré constant) using the generalized energy barrier $\bar{\epsilon}$ [Tem17, Definition 13]. Specifically, for any given $\beta > 0$, the spectral gap can be lower bounded by $C_N \exp(-\beta \bar{\epsilon})$, where C_N is a technical constant that typically scales as $1/N$. Although these works address thermalization across all temperatures, these lower bounds on the spectral gap are insufficient for efficiently preparing low-temperature thermal states, as the gap decays exponentially in β . Specifically, when using a local Davies generator to transition between ground states along a local Pauli path, the energy must first increase, requiring the dynamics to overcome the energy barrier to fully thermalize. Furthermore, as analyzed in [Tem17, KKCG24], an exponentially small spectral gap of order $\exp(-\Theta(\beta))$ in a local Davies generator appears inevitable when such energy barriers are present.

In our work, to overcome the bottleneck posed by the energy barrier, we modify the local Davies generator by incorporating appropriate global coupling operators that can directly connect the degenerate ground states, thereby avoiding the issues associated with the generalized energy barrier defined by local Pauli paths. By refining the analysis in [AFH09], we demonstrate that the resulting dynamics exhibits a spectral gap that decays polynomially with the size of the system but remains *independent of* β , ensuring fast mixing even at low temperatures. We note that the polynomially decaying spectral gap primarily arises from the mixing rate within the syndrome space, which remains unaffected by the introduction of the new global jump operators acting on the logical space. Consequently, our refined mixing time estimate rigorously demonstrates that the local Davies generator at low temperatures (and even at zero temperature) can efficiently annihilate quasi-particles residing in the syndrome space. A similar phenomenon has been numerically observed in the study of quantum memory [FHGW14, BLP⁺16, Fre18].

There is extensive literature on the mixing properties of local Davies generators for general local commuting Hamiltonians [KB16, BCG⁺23, KACR24, BCG⁺24]. However, most studies consider a fixed finite temperature $\beta = \mathcal{O}(1)$ [KB16, BCG⁺23, BCG⁺24, KACR24], particularly in the context of 1D local commuting Hamiltonians, where the mixing time implicitly depends on β , or a high temperature $\beta \ll 1$ [KB16, KACR24]. Extending these general approaches to low-temperature thermal state preparation and explicitly calculating the temperature dependence remains an interesting and challenging problem.

There is also a long line of works studying the fast mixing and rapid mixing of different types of classical Markov chains for spin systems. However, many classical results suffer from *low-temperature bottlenecks*: the dynamics can mix in polynomial time only when the inverse temperature β is below some threshold β_c . For example, it is well-known that the Glauber dynamics for the ferromagnetic Ising model with N spins on a d -dimensional lattice has mixing time $\Theta(N \log N)$ when $\beta < \beta_c(d)$ [MO94, LS16], and $e^{\Theta(N^{1-1/d})}$ when $\beta > \beta_c(d)$ [Pis96], where N is the total number of spins and the constant in the Θ notation depends on β . Some classical results managed to overcome this bottleneck by carefully designing the initial distribution [GS22], or studying other Markov chains or other graphical models

[JS93, GJ17, GŠV19, HPR19, BCP⁺21, CGG⁺21]. However, we note that these classical techniques cannot be applied directly to obtain our results.

1.4 Organization

In the following part of the paper, we start with a brief introduction to the Davies generator and properties of its spectral gap in Section 2. A technical overview of the proof of Theorem 1 is provided in Section 3. The detailed introduction to the 2D toric code and its proof can be found in Section 4. Additionally, in Appendix A, we discuss a simpler case of the 1D ferromagnetic Ising chain for completeness.

Acknowledgment

This material is partially supported by the U.S. Department of Energy, Office of Science, National Quantum Information Science Research Centers, Quantum Systems Accelerator (Z.D.), by the Challenge Institute for Quantum Computation (CIQC) funded by National Science Foundation (NSF) through grant number OMA-2016245 (L.L.), and by DOE Grant No. DE-SC0024124 (R.Z.). L.L. is a Simons Investigator in Mathematics. We thank Garnet Chan, Li Gao, Yunchao Liu, John Preskill for helpful discussions and feedbacks.

2 Preliminaries

Let H be a quantum many-body Hamiltonian on $\mathcal{H} \cong \mathbb{C}^{2^N}$ and $\sigma_\beta = e^{-\beta H} / \mathcal{Z}_\beta$ be the associated thermal state, where β is the inverse temperature and $\mathcal{Z}_\beta = \text{Tr}(e^{-\beta H})$ is the partition function. In this section, we shall recall the canonical form of the Davies generator with σ_β being the invariant state and some basic facts for its spectral gap analysis.

A superoperator $\Phi : \mathcal{B}(\mathcal{H}) \rightarrow \mathcal{B}(\mathcal{H})$ is a quantum channel if it is completely positive and trace preserving (CPTP). Lindblad dynamics is a C_0 -semigroup of quantum channels with the generator defined by $\mathcal{L}^\dagger(\rho) := \lim_{t \rightarrow 0^+} t^{-1}(\mathcal{P}_t^\dagger(\rho) - \rho)$ for $\rho \in \mathcal{D}(\mathcal{H})$. Here and in what follows, we adopt the convention that the adjoint operators (i.e., those with \dagger) are the maps in Schrödinger picture acting on quantum states. Both generators \mathcal{L} and \mathcal{L}^\dagger are usually referred to as Lindbladian. Davies generator is a special class of Lindbladians derived from the weak coupling limit of open quantum dynamics with a large thermal bath.

We first introduce the Bohr frequencies of H by

$$B_H := \{\omega = \lambda_i - \lambda_j : \forall \lambda_i, \lambda_j \in \text{Spec}(H)\},$$

where $\text{Spec}(H)$ is the spectral set of H . Let $\{S_a\}_{a \in \mathcal{A}}$ be a set of coupling operators with \mathcal{A} being a finite index set that satisfies

$$\{S_a\}_{a \in \mathcal{A}} = \{S_a^\dagger\}_{a \in \mathcal{A}}. \quad (2.1)$$

The jump operators $\{S_a(\omega)\}_{a, \omega}$ for the Davies generator are given by the Fourier components of the Heisenberg evolution of S_a :

$$e^{iHt} S_a e^{-iHt} = \sum_{\omega \in B_H} e^{i\omega t} \sum_{\lambda_i - \lambda_j = \omega} P_i S_a P_j := \sum_{\omega \in B_H} e^{i\omega t} S_a(\omega). \quad (2.2)$$

where $P_{i/j}$ is the projection into the eigenspace $\lambda_{i/j}$. By (2.1), we have $S_a(\omega)^\dagger = S_a(-\omega)$ for any $\omega \in B_H$.

We then introduce the Davies generator in the Heisenberg picture:

$$\mathcal{L}_\beta(X) := \sum_{a \in \mathcal{A}} \mathcal{L}_{S_a}(X), \quad X \in \mathcal{B}(\mathcal{H}), \quad (2.3)$$

with

$$\mathcal{L}_{S_a}(X) := \sum_{\omega \in B_H} \gamma_a(\omega) \left(S_a(\omega)^\dagger X S_a(\omega) - \frac{1}{2} \left\{ S_a(\omega)^\dagger S_a(\omega), X \right\} \right), \quad (2.4)$$

where the transition rate function $\gamma_a(\omega) > 0$ is given by the Fourier transform of the bath auto-correlation function satisfying the KMS condition [KFGV77]:

$$\gamma_a(-\omega) = e^{\beta\omega} \gamma_a(\omega).$$

In this work, we always choose the transition rate function $\gamma_a(\omega)$ as the Glauber form:

$$\gamma_a(\omega) = \frac{2}{e^{\beta\omega} + 1}, \quad (2.5)$$

For later use, we define $g_a(\omega) := e^{\beta\omega/2} \gamma_a(\omega)$ and find $g_a(\omega) = g_a(-\omega)$. Then, letting

$$L_a(\omega) = \sqrt{g_a(\omega)} S_a(\omega), \quad (2.6)$$

we reformulate the Davies generator (2.3)–(2.4) as follows:

$$\begin{aligned} \mathcal{L}_\beta(X) &= \sum_{a \in \mathcal{A}} \sum_{\omega \in B_H} e^{-\beta\omega/2} \left(L_a(\omega)^\dagger X L_a(\omega) - \frac{1}{2} \left\{ L_a(\omega)^\dagger L_a(\omega), X \right\} \right) \\ &= \frac{1}{2} \sum_{a \in \mathcal{A}} \sum_{\omega \in B_H} e^{-\beta\omega/2} L_a(\omega)^\dagger [X, L_a(\omega)] + e^{\beta\omega/2} [L_a(\omega), X] L_a(\omega)^\dagger \\ &= \frac{1}{2} \sum_{a \in \mathcal{A}} \sum_{\omega \in B_H} \gamma_a(\omega) S_a(\omega)^\dagger [X, S_a(\omega)] + \gamma_a(-\omega) [S_a(\omega), X] S_a(\omega)^\dagger. \end{aligned} \quad (2.7)$$

where the second step follows from

$$L_a(\omega)^\dagger = e^{\beta\omega/4} \sqrt{\gamma_a(\omega)} S_a(-\omega) = e^{\beta\omega/4} \sqrt{e^{-\beta\omega} \gamma_a(-\omega)} S_a(-\omega) = L_a(-\omega).$$

We now define the GNS inner product associated with the Gibbs state σ_β :

$$\langle Y, X \rangle_{\sigma_\beta} = \text{Tr}(Y^\dagger X \sigma_\beta). \quad (2.8)$$

It is known [KFGV77, DLL24] that the Davies generator satisfies the GNS detailed balance:

$$\langle Y, \mathcal{L}_\beta(X) \rangle_{\sigma_\beta} = \langle \mathcal{L}_\beta(Y), X \rangle_{\sigma_\beta},$$

and thus the associated Lindblad dynamics $e^{t\mathcal{L}_\beta^\dagger}$ admits σ_β as an invariant state, i.e.,

$$\mathcal{L}_\beta^\dagger(\sigma_\beta) = 0.$$

It follows that \mathcal{L}_β is similar to a self-adjoint operator for the HS inner product, called the *master Hamiltonian*, and has only real spectrum. To be precise, we introduce the transform $\varphi_X := X\sigma_\beta^{1/2}$, which gives $\langle Y, X \rangle_{\sigma_\beta} = \langle \varphi_Y, \varphi_X \rangle$. Then, the master Hamiltonian $\tilde{\mathcal{L}}_\beta$ is given by the similar transform of \mathcal{L}_β via φ_X :

$$\tilde{\mathcal{L}}_\beta := \varphi \circ \mathcal{L}_\beta \circ \varphi^{-1}, \quad (2.9)$$

satisfying $\langle Y, \mathcal{L}_\beta(X) \rangle_{\sigma_\beta} = \langle \varphi_Y, \tilde{\mathcal{L}}_\beta \varphi_X \rangle$. It is easy to see that $-\tilde{\mathcal{L}}_\beta$ is positive semi-definite and $\sqrt{\sigma_\beta}$ is the zero-energy ground state of $-\tilde{\mathcal{L}}_\beta$. Thus, the spectral gap of \mathcal{L}_β is the same as the ground state spectral gap of the Hamiltonian $-\tilde{\mathcal{L}}_\beta$.

We say that \mathcal{L}_β is primitive if σ_β is the unique invariant state; equivalently, the kernel $\ker(\mathcal{L}_\beta)$ is of one dimension, spanned by $\mathbf{1}$. In this case, we have

$$\lim_{t \rightarrow \infty} e^{t\mathcal{L}_\beta^\dagger}(\rho) = \sigma_\beta, \quad \forall \rho \in \mathcal{D}(\mathcal{H}),$$

and the spectral gap $\text{Gap}(\mathcal{L}_\beta)$ of the primitive Davies generator can be characterized by the variational form:

$$\text{Gap}(\mathcal{L}_\beta) = \inf_{X \neq 0, \text{Tr}(\sigma_\beta X) = 0} \frac{\langle X, \mathcal{L}_\beta(X) \rangle_{\sigma_\beta}}{\langle X, X \rangle_{\sigma_\beta}}.$$

Moreover, thanks to the detailed balance, the operator norm of \mathcal{L}_β can be computed by

$$\|\mathcal{L}_\beta\|_{\sigma_\beta \rightarrow \sigma_\beta} = \sup_{X \neq 0} \frac{\langle X, \mathcal{L}_\beta(X) \rangle_{\sigma_\beta}}{\langle X, X \rangle_{\sigma_\beta}}.$$

By [Wol12, ZB23], a sufficient and necessary condition for the primitivity of \mathcal{L}_β is the \mathbb{C} -algebra generated by all the jump operators $\{S_a(\omega)\}_{a,w}$ is the whole algebra $\mathcal{B}(\mathcal{H})$. By this condition, one can check that for the choice of $\{S_a\}_{a \in \mathcal{A}} = \{\sigma_i^x, \sigma_i^y, \sigma_i^z\}_{i=1}^N$, the associated Davies generator is always primitive. Without loss of generality, when discussing the Gibbs samplers in Appendix A and Section 4, we always let $\{\sigma_i^x, \sigma_i^y, \sigma_i^z\}_{i=1}^N$ be a subset of $\{S_a\}_{a \in \mathcal{A}}$ to guarantee the primitivity.

The following lemmas are collected from [AFH09, Lemmas 1 and 2] with proof omitted, which shall be used repeatedly in our subsequent spectral gap analysis.

Lemma 3. *Let $A, B \in \mathcal{B}(\mathcal{H})$ be positive operators on a Hilbert space \mathcal{H} , i.e., $A, B \geq 0$. The spectral gaps of A and B are their smallest non-zero positive eigenvalues, denoted by $\text{Gap}(A)$ and $\text{Gap}(B)$, respectively. We have:*

- If A has a non-trivial kernel and $A^2 \geq gA$ for some real $g > 0$, then

$$\text{Gap}(A) \geq g. \quad (2.10)$$

- If $\ker(A + B)$ is non-trivial such that $\ker(A + B) = \ker(B)$, then

$$\text{Gap}(A + B) \geq \text{Gap}(B). \quad (2.11)$$

- If A and B are commuting and $\ker(A + B)$ is non-trivial, then

$$\text{Gap}(A + B) \geq \min\{\text{Gap}(A), \text{Gap}(B)\}. \quad (2.12)$$

- If A has gap lower bound g_A and $\langle \varphi, B\varphi \rangle \geq g_B$ for all normalized $\varphi \in \ker(A)$, then

$$A + B \succeq \frac{g_A g_B}{g_A + \|B\|}, \quad (2.13)$$

where $\|B\|$ denotes the operator norm of B .

Remark 4. The second statement in Lemma 3 means that for any primitive Davies generator with σ_β being invariant, adding any other Davies generator keeping the invariant state can only increase the spectral gap.

3 Technical overview

In this section, we provide a technical overview of the proof of Theorem 1. In the analysis, there are three main steps:

- Decompose \mathcal{H} into logic and syndrome subspaces and the observable algebra $\mathcal{B}(\mathcal{H})$ correspondingly.
- Demonstrate efficient transition between logic subspaces.
- Demonstrate fast mixing inside the syndrome subspace.

The decomposition in the first step leverages the special structure of the stabilizer Hamiltonian, following the approach outlined in previous work by [AFH09]. Specifically, for the 2D toric code, we decompose $\mathcal{H} = \mathcal{H}_{\text{logic}} \otimes \mathcal{H}_{\text{syndrome}}$ according to the eigendecomposition of H^{toric} . Since H^{toric} has a four-dimensional ground state space, it encodes two logical qubits, making $\dim(\mathcal{H}_{\text{logic}}) = 4$. The syndrome subspace $\mathcal{H}_{\text{syndrome}}$ is then spanned by the electric and magnetic excited states, which are characterized by the bond configurations of the local observables in H^{toric} . That is, it can be further decomposed into the electric and magnetic excited subspaces $\mathcal{H}_{\text{syndrome}} = \mathcal{H}_{\text{b}}^{\text{m}} \otimes \mathcal{H}_{\text{b}}^{\text{e}}$. According to the decomposition of \mathcal{H} , we can naturally decompose the observable algebra $\mathcal{B}(\mathcal{H}) = \mathcal{Q}_1 \otimes \mathcal{Q}_2 \otimes \mathcal{A}_{\text{m}}^{\text{full}} \otimes \mathcal{A}_{\text{e}}^{\text{full}}$, where $\mathcal{Q}_1 \otimes \mathcal{Q}_2$ is generated by the logical operators, i.e., the global operators X_1, Z_1, X_2, Z_2 appearing in (1.1). The syndrome algebras $\mathcal{A}_{\text{m}}^{\text{full}}$ and $\mathcal{A}_{\text{e}}^{\text{full}}$ are spanned by linear transformations acting on the syndrome subspaces $\mathcal{H}_{\text{b}}^{\text{m}}$ and $\mathcal{H}_{\text{b}}^{\text{e}}$, respectively. Here, the \otimes symbol represents multiplication between commuting matrices, and every element in $\mathcal{Q}_1, \mathcal{Q}_2, \mathcal{A}_{\text{m}}^{\text{full}}$, and $\mathcal{A}_{\text{e}}^{\text{full}}$ is understood as a matrix defined over the entire Hilbert space \mathcal{H} . We put the detailed discussion of the above decomposition in Section 4.1.

After decomposing $\mathcal{B}(\mathcal{H})$, we can further decompose the Davies generator (1.1):

$$\mathcal{L}_\beta = \underbrace{\mathcal{L}_{\text{local}} + \mathcal{L}_{\text{global}}}_{:= \mathcal{L}^{\text{gapped}}} + \mathcal{L}^{\text{rest}},$$

with $\mathcal{L}^{\text{gapped}}$ defined in (4.13) and $\mathcal{L}^{\text{rest}} = \mathcal{L}_{\text{local full}} - \mathcal{L}_{\text{local}}$. Here we can show that $\mathcal{L}^{\text{gapped}}$ is ergodic, i.e., $\text{Ker}(\mathcal{L}^{\text{gapped}}) = \text{Span}\{\mathbf{1}\}$. By Lemma 3 (item 2), we can lower bound $\text{Gap}(\mathcal{L}_\beta)$ by $\text{Gap}(\mathcal{L}^{\text{gapped}})$. More importantly, the generator $\mathcal{L}^{\text{gapped}}$ is block diagonal with respect to the following decomposition:

$$\mathcal{B}(\mathcal{H}) = \bigoplus_{B_1 \in \{\mathbf{1}, X_1, Y_1, Z_1\}, B_2 \in \{\mathbf{1}, X_2, Y_2, Z_2\}} \mathcal{B}_{B_1, B_2},$$

where $\mathcal{B}_{B_1, B_2} = B_1 \otimes B_2 \otimes \mathcal{A}_m^{\text{full}} \otimes \mathcal{A}_e^{\text{full}}$ and the operators X_i, Y_i, Z_i are given in (4.4). Because $\text{Ker}(\mathcal{L}^{\text{gapped}}) = \text{Span}\{\mathbf{1}\}$ and $\mathcal{L}^{\text{gapped}}$ is block diagonal, we have

$$\begin{aligned} \text{Gap}(-\mathcal{L}_\beta) &\geq \text{Gap}(-\mathcal{L}^{\text{gapped}}) \\ &\geq \min \left\{ \text{Gap}(-\mathcal{L}^{\text{gapped}}|_{\mathcal{B}_{1,1}}), \lambda_{\min}(-\mathcal{L}^{\text{gapped}}|_{\mathcal{B}_{B_1, B_2}}) \Big| B_1 \neq \mathbf{1} \text{ or } B_2 \neq \mathbf{1} \right\}. \end{aligned} \quad (3.1)$$

Thus, for a lower bound estimate of $\text{Gap}(-\mathcal{L}^{\text{gapped}})$, it suffices to consider $\text{Gap}(-\mathcal{L}^{\text{gapped}}|_{\mathcal{B}_{1,1}})$ and $\lambda_{\min}(-\mathcal{L}^{\text{gapped}}|_{\mathcal{B}_{B_1, B_2}})$ with $B_1 \neq \mathbf{1}$ or $B_2 \neq \mathbf{1}$. The latter term characterizes the transition rate between different logical subspaces. If \mathcal{L}_β contains only local coupling operators, the system requires a long evolution time to overcome the energy barrier and transit between different logical subspaces, which leads to a slow mixing time scaling as $\exp(\Theta(\beta))$ according to [AFH09]. In our work, an important observation is that the global logical operators X_1, Z_1, X_2, Z_2 can directly flip the logical qubits, enabling transitions between different logical subspaces without the need to overcome the energy barrier. The efficient transition in logic density space implies a fast decaying of $\exp(t\mathcal{L}^{\text{gapped}})$ in the logic subspace $\{\mathcal{B}_{B_1, B_2}\}_{B_1 \neq \mathbf{1} \text{ or } B_2 \neq \mathbf{1}}$ and a lower bound of $\{-\mathcal{L}^{\text{gapped}}|_{\mathcal{B}_{B_1, B_2}}\}_{B_1 \neq \mathbf{1} \text{ or } B_2 \neq \mathbf{1}}$. Specifically, in Proposition 8 in Section 4.2, we show

$$-\mathcal{L}^{\text{gapped}}|_{\mathcal{B}_{B_1, B_2}} \succeq \text{Gap}(-\mathcal{L}_{\text{local}}|_{\mathcal{B}_{1,1}}). \quad (3.2)$$

According to the above analysis, the remaining thing to lower bound the spectral gap of \mathcal{L}_β is to study the spectral gap of $\mathcal{L}_{\text{local}}$ on $\mathcal{B}_{1,1}$. Roughly speaking, this requires us to prove Proposition 2. Similar task is done in [AFH09]. However, we emphasize that the lower bound and proof technique in [AFH09] is **not** suitable for our purpose. In [AFH09, Proposition 2], while the spectral gap is independent of the system size, it decays as $\exp(-\Theta(\beta))$, indicating slow mixing in the syndrome subspace at low temperatures. A main contribution of this work is to show that this lower bound is not tight when $\beta \gg 1$, and the system actually mixes fast in the syndrome subspace at low temperatures. To this end, we develop a new iteration argument and a decomposition trick to prove that $\text{Gap}(\mathcal{L}_{\text{local}}|_{\mathcal{B}_{1,1}}) \geq \min\{\exp(-\Theta(\beta)), \text{poly}(1/N)\}$, which provides a much sharper lower bound of the spectral gap in the lower temperature regime. This result is summarized in Proposition 9 in Section 4.2.1, which also provides a proof of Proposition 2. Plugging this into (3.1) and (3.2), we can conclude Theorem 1.

4 2D toric code

Let $N = 2L^2$ spins be on the edges of the toroidal lattice, modeled by the Hilbert space $\mathcal{H} \cong \mathbb{C}^{2^N}$. The Hamiltonian is given by

$$H^{\text{toric}} = - \sum_s \mathbf{X}_s - \sum_p \mathbf{Z}_p, \quad (4.1)$$

where indices s and p denote a *star* and *plaquette* that consist of four sites around a node of the lattice and the center of a cell, respectively, as drawn in Fig. 1, and the associated observables \mathbf{X}_s and \mathbf{Z}_p are given by

$$\mathbf{X}_s = \prod_{i \in s} \sigma_i^x, \quad \mathbf{Z}_p = \prod_{i \in p} \sigma_i^z,$$

which commute with each other: $[\mathbf{X}_s, \mathbf{Z}_p] = [\mathbf{X}_s, \mathbf{X}_{s'}] = [\mathbf{Z}_p, \mathbf{Z}_{p'}] \equiv 0$ for any stars s, s' and plaquettes p, p' . In addition, due to the periodic boundary condition, it holds that

$$\prod_s \mathbf{X}_s = 1, \quad \prod_p \mathbf{Z}_p = 1, \quad (4.2)$$

This section is devoted to the spectral gap analysis of the Davies generator (Gibbs sampler) in (1.1) and the proof of Theorem 1, building on the discussion in Section 3. We will first discuss the ground states and the decomposition of the observable algebra of H^{toric} in Section 4.1. Then, in Section 4.2, we first address the step (b) outlined in Section 3, reducing the problem to step (c): the study of the spectral gap of the local Davies generator on the syndrome space. This will be explored in detail in Section 4.2.1.

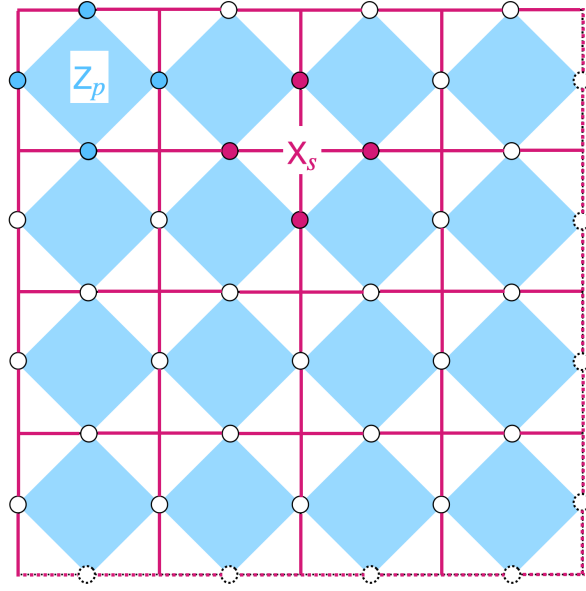


Figure 1: 2D toric code. Each blue plaquette contains one 4-local operator $\mathbf{Z}_p = \prod_{i \in \text{plaquette } p} \sigma_i^z$. Each red star contains one 4-local operator $\mathbf{X}_s = \prod_{i \in \text{star } s} \sigma_i^x$. The dashed line on the right/bottom is the same as the solid line on the left/up to indicate the periodic boundary condition.

4.1 Ground states and observable algebra

In this section, we introduce the ground state space of H^{toric} and the associated observable algebra $\mathcal{B}(\mathcal{H})$, following [AFH09, AHHH10, Bom13], which is important for the step (a) of the road map in Section 3.

Analogous to the 1D ferromagnetic Ising chain (see Appendix A), the 2D toric code Hamiltonian H^{toric} is frustration-free, i.e., its ground state is simultaneously an eigenvector with eigenvalue 1 for all local terms \mathbf{X}_s and \mathbf{Z}_p . Due to the toric structure with periodic boundary conditions, there are two topologically protected degrees of freedom (i.e., two logical qubits), resulting in a four-dimensional ground state space.

We now construct the ground state space of H^{toric} explicitly. Given a vector $|\phi\rangle$ satisfying $\mathbf{Z}_p |\phi\rangle = |\phi\rangle$ for all p , e.g., $|0^N\rangle$ or $|1^N\rangle$ (note that there are many others), we can construct a ground state as follows:

$$|\psi\rangle = \mathbf{X}_{\text{star}} |\phi\rangle, \quad \mathbf{X}_{\text{star}} := \prod_{s \in \text{star}} (I + \mathbf{X}_s) = \sum_{\alpha \in \{0,1\}^N} \prod_{s \in \text{star}} \mathbf{X}_s^{\alpha_s}, \quad (4.3)$$

which, as one can easily check, satisfies $\mathbf{Z}_p |\psi\rangle = |\psi\rangle$, $\mathbf{X}_s |\psi\rangle = |\psi\rangle$ for all p, s . To find all the ground states, we first define some global observables for two logical qubits (see Fig. 2):

$$\begin{aligned} \mathbf{X}_1 &:= \prod_{j \in \text{orange dots}} \sigma_j^x, & \mathbf{Z}_1 &:= \prod_{j \in \text{green squares}} \sigma_j^z, & \mathbf{Y}_1 &:= i\mathbf{Z}_1\mathbf{X}_1, \\ \mathbf{X}_2 &:= \prod_{j \in \text{blue dots}} \sigma_j^x, & \mathbf{Z}_2 &:= \prod_{j \in \text{red squares}} \sigma_j^z, & \mathbf{Y}_2 &:= i\mathbf{Z}_2\mathbf{X}_2. \end{aligned} \quad (4.4)$$

Here, $\{\mathbf{X}_1, \mathbf{Y}_1, \mathbf{Z}_1\}$ and $\{\mathbf{X}_2, \mathbf{Y}_2, \mathbf{Z}_2\}$ generates two commuting Pauli algebras. Moreover, the operators \mathbf{X}_1 and \mathbf{X}_2 give one-to-one correspondences between four topological equivalent classes [AHHH10, Fig. 3.2] (see also [Bom13, Section 3.2]). Specifically, we consider four orthogonal vectors that satisfy $\mathbf{Z}_p |\phi\rangle = |\phi\rangle$:

$$|\phi_o\rangle = |0^N\rangle, \quad |\phi_|\rangle = \mathbf{X}_1 |0^N\rangle, \quad |\phi_-\rangle = \mathbf{X}_2 |0^N\rangle, \quad |\phi_+\rangle = \mathbf{X}_1\mathbf{X}_2 |0^N\rangle.$$

They generate the four orthogonal ground states via (4.3):

$$|\psi_g\rangle = \mathbf{X}_{\text{star}} |\phi_g\rangle \quad \text{with} \quad g = o, |, -, +, \quad (4.5)$$

which span the whole ground state space of H^{toric} . In this form, $|\psi_g\rangle$ with $g = o, |, -, +$ corresponds to the logical qubits $|00\rangle$, $|10\rangle$, $|01\rangle$, and $|11\rangle$, respectively.

Next, to formulate the observable algebra, we first consider how the bit flip will influence the energy, namely, the excitation of H^{toric} . For this, we delicately construct a snake path (as a subset of $N = 2L^2$ sites) passing through the centers of all the cells and a comb path passing through all the nodes of the toroidal lattice (see Fig. 3) such that

- $\{\sigma_j^x\}_{j \in \text{snake}}$ generates all the X -type excitations (also called “magnetic” excitations): for any two plaquettes (p_1, p_2) , we can find a path l on the snake connecting them (blue path in Fig. 3). Then we define

$$W_l^m = \prod_{j \in l} \sigma_j^x, \quad (4.6)$$

and then have the excited state $|\psi_{p_1, p_2}\rangle = W_l^m |\psi\rangle$ satisfying

$$\mathbf{Z}_{p_1/p_2} |\psi_{p_1, p_2}\rangle = -|\psi_{p_1, p_2}\rangle, \quad H^{\text{toric}} |\psi_{p_1, p_2}\rangle = E_{\text{ground}} + 2,$$

where $|\psi\rangle$ is a ground state of H^{toric} .

- $\{\sigma_j^z\}_{j \in \text{comb}}$ generates all the Z -type excitations (also called “electric” excitations): for any two stars (s_1, s_2) , we can find a path l on the comb connecting them (red path in Fig. 3). We then define

$$W_l^e = \prod_{j \in l} \sigma_j^z. \quad (4.7)$$

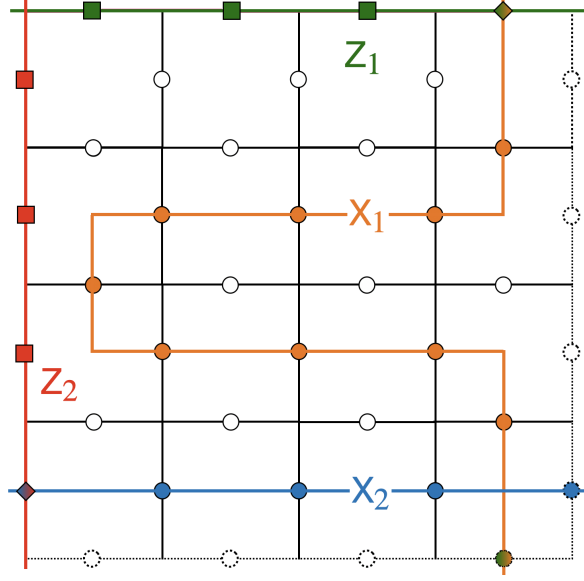


Figure 2: Four global logic operators in 2D toric code. Orange: $X_1 = \prod_{j \in \text{orange dots}} \sigma_j^x$. Green: $Z_1 = \prod_{j \in \text{green squares}} \sigma_j^z$. Blue: $X_2 = \prod_{j \in \text{blue dots}} \sigma_j^x$. Red: $Z_2 = \prod_{j \in \text{red squares}} \sigma_j^z$. Squares represent the qubits on Z_1, Z_2 logic operators, while dots represent the qubits on X_1, X_2 logic operators.

For a ground state $|\psi\rangle$, we define the excited state $|\psi_{s_1, s_2}\rangle = W_l^e |\psi\rangle$ satisfying

$$\mathbf{X}_{s_1/s_2} |\psi_{s_1, s_2}\rangle = -|\psi_{s_1, s_2}\rangle, \quad H^{\text{toric}} |\psi_{s_1, s_2}\rangle = E_{\text{ground}} + 2.$$

thanks to $\mathbf{X}_{s_1/s_2} W_l^e = -W_l^e \mathbf{X}_{s_1/s_2}$.

- The snake and comb form a partition of all but two spins. In addition, the snake does not intersect with Z_1, Z_2 , and the comb does not intersect with X_1, X_2 . This ensures that the excitation operators $W_l^{m/e}$ constructed above commute with global observables: for a ground state $|\psi\rangle$,

$$O W_l^{m/e} |\psi\rangle = W_l^{m/e} O |\psi\rangle,$$

where $O = X_1, X_2, Z_1$, and Z_2 .

These elementary excited states $|\psi_{p_1, p_2}\rangle, |\psi_{s_1, s_2}\rangle$ are often called quasi-particles pairs (or quasi-particles for short). All excited states of H^{toric} can be expressed using these quasi-particles.

Following the above discussions, we decompose the space \mathcal{H} according to the magnetic excitations observed by \mathbf{Z}_p and the electric excitations observed by \mathbf{X}_s :

$$\mathcal{H} = \mathbb{C}^2 \otimes \mathbb{C}^2 \otimes \mathcal{H}_b \cong \mathbb{C}^{2^{N=2L^2}} \quad \text{with} \quad \mathcal{H}_b = \mathcal{H}_b^m \otimes \mathcal{H}_b^e, \quad (4.8)$$

where $\mathcal{H}_b^{m/e}$ is the space of electric/magnetic excited states spanned by

$$\left\{ \prod_l W_l^{m/e} |\psi_g\rangle : W_l^{m/e} \text{ given in (4.6) and (4.7), } g = o, |, -, + \right\}. \quad (4.9)$$

Moreover, a basis vector in \mathcal{H}_b can be identified as

$$|m\rangle |e\rangle = |m_1, \dots, m_{L^2}\rangle |e_1, \dots, e_{L^2}\rangle \in \{+1, -1\}^{2L^2}, \quad (4.10)$$

such that $\#\{m_j = -1\}, \#\{e_j = -1\} \in 2\mathbb{Z}$, due to the periodic boundary condition, with $m_j = \pm 1$ (resp., $e_j = \pm 1$) denoting the observation under \mathbf{Z}_p (resp., \mathbf{X}_s). Here and in what follows, we sort $\{\mathbf{Z}_p\}_p$ and $\{\mathbf{X}_s\}_s$ along the snake and comb such that they can be indexed by $j \in \{1, \dots, L^2\}$ (see Fig. 3). We emphasize that $\dim(\mathcal{H}_b) = 2^{2L^2-2}$ follows from the parity constraint (4.2), while each $|m\rangle |e\rangle$ is a $2L^2$ -dimensional vector.

Now, we are ready to decompose the observable algebra $\mathcal{B}(\mathcal{H})$. Let \mathcal{Q}_1 and \mathcal{Q}_2 be the observable algebras over two logical qubits, generated by \mathbf{X}_1 and \mathbf{Z}_1 and by \mathbf{X}_2 and \mathbf{Z}_2 , respectively. We denote by $\mathcal{A}_{m/e}^{\text{full}}$ the linear operator spaces on $\mathcal{H}_b^{m/e}$. Then we have the following decomposition of the observable algebra for the 2D toric code. The proof is straightforward and given in Section 4.3 for completeness.

Lemma 5. *The algebra of observables for 2D toric code can be decomposed into*

$$\mathcal{B}(\mathcal{H}) \cong \mathcal{Q}_1 \otimes \mathcal{Q}_2 \otimes \mathcal{A}_m^{\text{full}} \otimes \mathcal{A}_e^{\text{full}}, \quad (4.11)$$

associated with the decomposition (4.8), where the algebras $\mathcal{A}_m^{\text{full}}$ and $\mathcal{A}_e^{\text{full}}$ are generated by $\{\mathbf{Z}_p\}_p \cup \{\sigma_j^x\}_{j \in \text{snake}}$ and $\{\mathbf{X}_s\}_s \cup \{\sigma_j^z\}_{j \in \text{comb}}$. In addition, the four subalgebras \mathcal{Q}_1 , \mathcal{Q}_2 , $\mathcal{A}_m^{\text{full}}$, and $\mathcal{A}_e^{\text{full}}$ are commutative with each other.

To give further interpretation on the decomposition (4.11), we define four subspaces \mathcal{H}_g with $g = o, |, -, +$ spanned by the ground state $|\psi_g\rangle$ in (4.5) and its excited states $W_l^{m/e} |\psi_g\rangle$ via (4.6) and (4.7). Then it is easy to see $\dim(\mathcal{H}_g) = 2^{N-2}$ with $N = 2L^2$. The algebra $\mathcal{Q}_1 \otimes \mathcal{Q}_2$ gives all the linear transformation between subspaces \mathcal{H}_g with $g = o, |, -, +$, while on each subspace \mathcal{H}_g , the linear maps are characterized by $\mathcal{A}_m^{\text{full}} \otimes \mathcal{A}_e^{\text{full}}$. In particular, recalling the basis (4.10), $\mathcal{A}_m^{\text{full}}$ (resp., $\mathcal{A}_e^{\text{full}}$) transfers the bond $|m\rangle$ (resp., $|e\rangle$), for example,

$$\mathcal{A}_m^{\text{full}}(|m\rangle |e\rangle) = \left(\mathcal{A}_m^{\text{full}} |m\rangle \right) |e\rangle.$$

4.2 Spectral gap of the Gibbs sampler

In this section, we will focus on steps (b) and (c) of the roadmap in Section 3. For this, we decompose the generator (1.1) as follows:

$$\mathcal{L}_\beta = \mathcal{L}_{\text{local full}} + \mathcal{L}_{\text{global}} = \mathcal{L}^{\text{gapped}} + \mathcal{L}^{\text{rest}}, \quad (4.12)$$

where

$$\mathcal{L}^{\text{gapped}} := \underbrace{\sum_{j \in \text{snake}} \mathcal{L}_{\sigma_j^x} + \sum_{j \in \text{comb}} \mathcal{L}_{\sigma_j^z}}_{:= \mathcal{L}_{\text{local}}} + \underbrace{\mathcal{L}_{\mathbf{X}_1} + \mathcal{L}_{\mathbf{X}_2} + \mathcal{L}_{\mathbf{Z}_1} + \mathcal{L}_{\mathbf{Z}_2}}_{:= \mathcal{L}_{\text{global}}}. \quad (4.13)$$

Here $\mathcal{L}^{\text{rest}} := \mathcal{L}_{\text{local full}} - \mathcal{L}_{\text{local}}$ is a local Lindbladian with other Pauli couplings not included in $\mathcal{L}_{\text{local}}$. From Lemma 3 (item 2), it suffices to limit our discussion to the part $\mathcal{L}^{\text{gapped}}$ and show that it is primitive with the desired spectral gap lower bound $\max\{\exp(-\mathcal{O}(\beta)), \Omega(N^{-3})\}$.

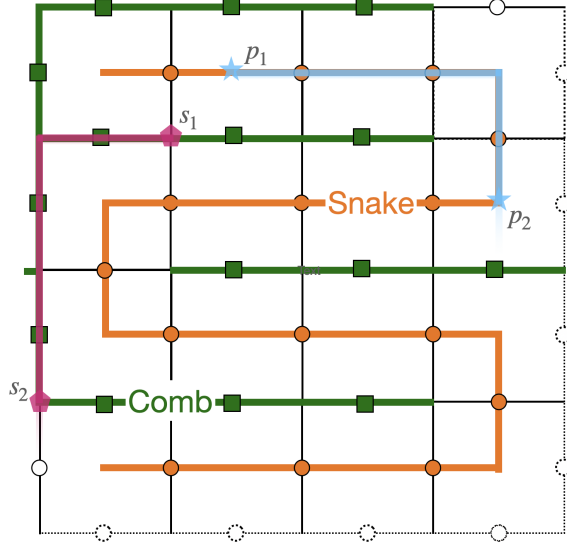


Figure 3: Orange dot Snake and green square comb for 2D toric code. The blue magnetic path operators W_l^m (4.6) and red electric path operators W_l^e (4.7) act along the snake and the comb, respectively. We index $\{\mathbf{Z}_p\}_p$ as $\{\mathbf{Z}_j\}_{j=1}^{L^2}$ along the snake from left to right and up to down, and index the spins from 2 to L^2 on the snake in the same way so that each spin j corresponds a pair of plaquettes $j-1$ and j . One can similarly index the stars and spins on comb from left to right and up to down.

Before we proceed, we prepare the explicit formulations of the Lindbladians involved in $\mathcal{L}^{\text{gapped}}$ for subsequent analysis. For σ_j^x with $j \in \text{snake}$, we have

$$e^{itH^{\text{toric}}} \sigma_j^x e^{-itH^{\text{toric}}} = e^{-it(\mathbf{Z}_{p'} + \mathbf{Z}_p)} \sigma_j^x e^{it(\mathbf{Z}_{p'} + \mathbf{Z}_p)},$$

where p and p' are the two plaquettes with $j = p \cap p'$ being the intersection site. The bond observable $-(\mathbf{Z}_{p'} + \mathbf{Z}_p)$ has eigenvalues $-2, 0, 2$ with the associated eigenprojections denoted by P_j^-, P_j^0, P_j^+ , respectively, which can be represented as follows:

$$P_j^0 = \frac{1}{2}(I - \mathbf{Z}_{p'} \mathbf{Z}_p), \quad P_j^\pm = \frac{1}{4}(I \mp \mathbf{Z}_{p'})(I \mp \mathbf{Z}_p). \quad (4.14)$$

We then compute the Fourier components of σ_j^x ($j \in \text{snake}$):

$$e^{itH^{\text{toric}}} \sigma_j^x e^{-itH^{\text{toric}}} = e^{-4it} \underbrace{P_j^- \sigma_j^x P_j^+}_{a_j} + e^{4it} \underbrace{P_j^+ \sigma_j^x P_j^-}_{a_j^\dagger} + \underbrace{P_j^0 \sigma_j^x P_j^0}_{a_j^0}, \quad (4.15)$$

due to $P_j^\pm \sigma_j^x P_j^0 = P_j^+ \sigma_j^x P_j^+ = P_j^- \sigma_j^x P_j^- = 0$, where a_j, a_j^\dagger, a_j^0 correspond to the Bohr frequencies $-4, 4, 0$ of the Hamiltonian (4.1), respectively. Then, we can write $\mathcal{L}_{\sigma_j^x}$ by Eqs. (2.3) and (2.7) with Glauber-type transition (2.5):

$$\begin{aligned} \mathcal{L}_{\sigma_j^x}(A) = & -\frac{1}{2}[a_j^0, [a_j^0, A]] + \frac{1}{2} \left\{ h_+ a_j^\dagger [A, a_j] + h_- [a_j, A] a_j^\dagger \right\} \\ & + \frac{1}{2} \left\{ h_+ [a_j^\dagger, A] a_j + h_- a_j [A, a_j^\dagger] \right\}, \quad (4.16) \end{aligned}$$

where the constants h_{\pm} are given by

$$h_+ = \gamma(-4) = \frac{2}{e^{-4\beta} + 1}, \quad h_- = \gamma(4) = \frac{2}{e^{4\beta} + 1}. \quad (4.17)$$

The computation for $\mathcal{L}_{\sigma_j^z}$ with $j \in \text{comb}$ is quite similar to $\mathcal{L}_{\sigma_j^x}$ with $j \in \text{snake}$, so we only sketch it below. For σ_j^z with $j \in \text{comb}$, we have

$$\begin{aligned} e^{itH^{\text{toric}}} \sigma_j^x e^{-itH^{\text{toric}}} &= e^{-it(\mathbf{X}_{s'} + \mathbf{X}_s)} \sigma_j^x e^{it(\mathbf{X}_{s'} + \mathbf{X}_s)} \\ &= e^{-4it} \underbrace{Q_j^- \sigma_j^z Q_j^+}_{b_j} + e^{4it} \underbrace{Q_j^+ \sigma_j^z Q_j^-}_{b_j^\dagger} + \underbrace{Q_j^0 \sigma_j^z Q_j^0}_{b_j^0}, \end{aligned}$$

with s and s' being two starts uniquely determined by $j = s \cap s'$. Here, the projections Q_j^- , Q_j^0 , Q_j^+ are the eigenprojections of the bond observable $-(\mathbf{X}_{s'} + \mathbf{X}_s)$ for eigenvalues $-2, 0, 2$, which can be similarly formulated as (4.14) by replacing \mathbf{Z}_p by \mathbf{X}_s . With the Glauber-type transition rate (2.5), the generator $\mathcal{L}_{\sigma_j^x}$ is given by

$$\begin{aligned} \mathcal{L}_{\sigma_j^z}(A) &= -\frac{1}{2} [b_j^0, [b_j^0, A]] + \frac{1}{2} \left\{ h_+ b_j^\dagger [A, b_j] + h_- [b_j, A] b_j^\dagger \right\} \\ &\quad + \frac{1}{2} \left\{ h_+ [b_j^\dagger, A] b_j + h_- b_j [A, b_j^\dagger] \right\}, \end{aligned} \quad (4.18)$$

where the constants h_{\pm} is the same as (4.17). According to our construction, we have

$$\|\mathcal{L}_{\sigma_j^z}\|_{\sigma_\beta \rightarrow \sigma_\beta}, \quad \|\mathcal{L}_{\sigma_j^x}\|_{\sigma_\beta \rightarrow \sigma_\beta} = \Theta(1), \quad \text{uniformly in } \beta.$$

We proceed to compute the Lindbladian with global couplings. For $\mathbf{O} = \mathbf{X}_1, \mathbf{X}_2, \mathbf{Z}_1, \mathbf{Z}_2$, thanks to $e^{itH^{\text{toric}}} \mathbf{O} e^{-itH^{\text{toric}}} = \mathbf{O}$ by $[\mathbf{Z}_p, \mathbf{O}] = [\mathbf{X}_s, \mathbf{O}] = 0$, we readily have

$$\mathcal{L}_{\mathbf{O}}(A) = -\frac{1}{2} [\mathbf{O}, [\mathbf{O}, A]], \quad (4.19)$$

since \mathbf{O} has only the component with Bohr frequency zero. It is clear that

$$\|\mathcal{L}_{\mathbf{O}}\|_{\sigma_\beta \rightarrow \sigma_\beta} = \Theta(1), \quad \text{uniformly in } \beta. \quad (4.20)$$

Now, for the step (b) of the roadmap in Section 3, we first give the following lemma. Its proof is postponed to Section 4.3 for ease of reading.

Lemma 6. *The generators $\mathcal{L}_{\text{global}}$, $\sum_{j \in \text{snake}} \mathcal{L}_{\sigma_j^x}$, and $\sum_{j \in \text{comb}} \mathcal{L}_{\sigma_j^z}$ defined in (4.13) only nontrivially act on a subalgebra of $\mathcal{B}(\mathcal{H})$. Specifically, we have*

$$\mathcal{L}_{\text{global}} \left(\mathcal{Q}_1 \otimes \mathcal{Q}_2 \otimes \mathcal{A}_m^{\text{full}} \otimes \mathcal{A}_e^{\text{full}} \right) = \mathcal{L}_{\text{global}} (\mathcal{Q}_1 \otimes \mathcal{Q}_2) \otimes \mathcal{A}_m^{\text{full}} \otimes \mathcal{A}_e^{\text{full}}, \quad (4.21)$$

$$\sum_{j \in \text{snake}} \mathcal{L}_{\sigma_j^x} \left(\mathcal{Q}_1 \otimes \mathcal{Q}_2 \otimes \mathcal{A}_m^{\text{full}} \otimes \mathcal{A}_e^{\text{full}} \right) = \mathcal{Q}_1 \otimes \mathcal{Q}_2 \otimes \sum_{j \in \text{snake}} \mathcal{L}_{\sigma_j^x} \left(\mathcal{A}_m^{\text{full}} \right) \otimes \mathcal{A}_e^{\text{full}}, \quad (4.22)$$

and

$$\sum_{j \in \text{comb}} \mathcal{L}_{\sigma_j^z} \left(\mathcal{Q}_1 \otimes \mathcal{Q}_2 \otimes \mathcal{A}_m^{\text{full}} \otimes \mathcal{A}_e^{\text{full}} \right) = \mathcal{Q}_1 \otimes \mathcal{Q}_2 \otimes \mathcal{A}_m^{\text{full}} \otimes \sum_{j \in \text{comb}} \mathcal{L}_{\sigma_j^z} \left(\mathcal{A}_e^{\text{full}} \right). \quad (4.23)$$

In particular, it holds that

$$\begin{aligned}
\text{Ker}\left(\sum_{j \in \text{snake}} \mathcal{L}_{\sigma_j^x}\right) &= \mathcal{Q}_1 \otimes \mathcal{Q}_2 \otimes \mathbf{1} \otimes \mathcal{A}_e^{\text{full}}, \\
\text{Ker}\left(\sum_{j \in \text{comb}} \mathcal{L}_{\sigma_j^z}\right) &= \mathcal{Q}_1 \otimes \mathcal{Q}_2 \otimes \mathcal{A}_m^{\text{full}} \otimes \mathbf{1}, \\
\text{Ker}(\mathcal{L}_{\text{global}}) &= \mathbf{1} \otimes \mathbf{1} \otimes \mathcal{A}_m^{\text{full}} \otimes \mathcal{A}_e^{\text{full}}.
\end{aligned} \tag{4.24}$$

Note from (4.19) that for any $B_1, B_2 \in \{I, X_i, Y_i, Z_i\}$, the operator $B_1 B_2$ is an eigenvector of $\mathcal{L}_{\text{global}}$: $\mathcal{L}_{\text{global}}(B_1 B_2) = c \cdot B_1 B_2$ for some constant c . Combining this with Lemma 6, we obtain the following properties of $\mathcal{L}^{\text{gapped}}$.

Corollary 7. *It holds that*

- $\mathcal{L}^{\text{gapped}}$ is block diagonal for the following orthogonal decomposition (4.25) in both HS inner product and GNS inner product:

$$\mathcal{Q}_1 \otimes \mathcal{Q}_2 \otimes \mathcal{A}_m^{\text{full}} \otimes \mathcal{A}_e^{\text{full}} = \bigoplus_{B_i \in \{I, X_i, Y_i, Z_i\}, i=1,2} \mathcal{B}_{B_1, B_2}, \tag{4.25}$$

with

$$\mathcal{B}_{B_1, B_2} = B_1 \otimes B_2 \otimes \mathcal{A}_m^{\text{full}} \otimes \mathcal{A}_e^{\text{full}}.$$

- $\mathcal{L}^{\text{gapped}}$ is primitive: $\text{Ker}(\mathcal{L}^{\text{gapped}}) = \text{Span}\{\mathbf{1}\}$.

By (2.11) in Lemma 3 with the primitivity of $\mathcal{L}^{\text{gapped}}$, we have

$$\text{Gap}(-\mathcal{L}_\beta) = \text{Gap}(-\mathcal{L}^{\text{rest}} - \mathcal{L}^{\text{gapped}}) \geq \text{Gap}(-\mathcal{L}^{\text{gapped}}).$$

Further, from the block diagonal form of $\mathcal{L}^{\text{gapped}}$ for (4.25), we obtain (3.1):

$$\begin{aligned}
\text{Gap}(-\mathcal{L}_\beta) &\geq \text{Gap}(-\mathcal{L}^{\text{gapped}}) \\
&\geq \min \left\{ \text{Gap}(-\mathcal{L}^{\text{gapped}}|_{\mathcal{B}_{1,1}}), \lambda_{\min}(-\mathcal{L}^{\text{gapped}}|_{\mathcal{B}_{B_1, B_2}}) \text{ for } B_1 \neq \mathbf{1} \text{ or } B_2 \neq \mathbf{1} \right\}.
\end{aligned} \tag{4.26}$$

For the first term in (4.26), we note that $\mathcal{L}_{\text{global}}|_{\mathcal{B}_{1,1}} = 0$ from (4.24), and then have

$$\text{Gap}(-\mathcal{L}^{\text{gapped}}|_{\mathcal{B}_{1,1}}) = \text{Gap}(-\mathcal{L}_{\text{local}}|_{\mathcal{B}_{1,1}}). \tag{4.27}$$

We next consider the lower bound estimation of $\lambda_{\min}(-\mathcal{L}^{\text{gapped}}|_{\mathcal{B}_{B_1, B_2}})$. For any $B_i \in \{I, X_i, Y_i, Z_i\}$ with $i = 1, 2$ such that $B_1 \neq \mathbf{1}$ or $B_2 \neq \mathbf{1}$, the operators X_1, X_2, Z_1, Z_2 either commute or anti-commute with $B_1 B_2$, and there always exists one, say O , among them that anti-commutes with $B_1 B_2$. Then, by (4.19), we have $\mathcal{L}_O(A) = -2A$, which implies

$$\langle B_1 B_2, -\mathcal{L}_{\text{global}}(B_1 B_2) \rangle_{\sigma_\beta} \geq \langle B_1 B_2, -\mathcal{L}_O(B_1 B_2) \rangle_{\sigma_\beta} = 2. \tag{4.28}$$

Furthermore, according to Eqs. (4.22) to (4.24) in Lemma 6, we find

$$\text{Ker}(\mathcal{L}_{\text{local}}|_{\mathcal{B}_{B_1, B_2}}) = B_1 B_2.$$

Finally, by Lemma 3 (item 4), there holds

$$\begin{aligned} -\mathcal{L}^{\text{gapped}}|_{\mathcal{B}_{B_1, B_2}} &\succeq \frac{\text{Gap}\left(\mathcal{L}_{\text{local}}|_{\mathcal{B}_{B_1, B_2}}\right) \langle B_1 B_2, -\mathcal{L}_{\text{global}}(B_1 B_2) \rangle_{\sigma_\beta}}{\text{Gap}\left(\mathcal{L}_{\text{local}}|_{\mathcal{B}_{B_1, B_2}}\right) + \|\mathcal{L}_{\text{global}}\|_{\sigma_\beta \rightarrow \sigma_\beta}} \\ &= \Theta\left(\frac{\text{Gap}\left(\mathcal{L}_{\text{local}}|_{\mathcal{B}_{B_1, B_2}}\right)}{\text{Gap}\left(\mathcal{L}_{\text{local}}|_{\mathcal{B}_{B_1, B_2}}\right) + 1}\right), \end{aligned} \quad (4.29)$$

where we have used (4.20). Plugging this into (4.26), we obtain the following proposition, concluding step (b) of the proof.

Proposition 8. *Let \mathcal{L}_β , $\mathcal{L}^{\text{gapped}}$, $\mathcal{L}_{\text{global}}$ and $\mathcal{L}_{\text{local}}$ be defined in (4.12)-(4.13). Suppose $\text{Gap}(\mathcal{L}_{\text{local}}|_{\mathcal{B}_{1,1}}) = \mathcal{O}(1)$. Then, for any $B_i \in \{I, X_i, Y_i, Z_i\}$ with $i = 1, 2$ such that $B_1 \neq \mathbf{1}$ or $B_2 \neq \mathbf{1}$, we have*

$$-\mathcal{L}^{\text{gapped}}|_{\mathcal{B}_{B_1, B_2}} \succeq \Omega\left(\text{Gap}(\mathcal{L}_{\text{local}}|_{\mathcal{B}_{1,1}})\right), \quad (4.30)$$

Moreover, it holds that

$$\text{Gap}(\mathcal{L}_\beta) = \Omega\left(\text{Gap}(-\mathcal{L}_{\text{local}}|_{\mathcal{B}_{1,1}})\right). \quad (4.31)$$

Proof. Since the action of $\mathcal{L}_{\text{local}}$ on \mathcal{B}_{B_1, B_2} is independent of B_1, B_2 by (4.22) and (4.23), we obtain $\text{Gap}(\mathcal{L}_{\text{local}}|_{\mathcal{B}_{B_1, B_2}}) = \text{Gap}(\mathcal{L}_{\text{local}}|_{\mathcal{B}_{1,1}})$, which, along with (4.29), implies (4.30). Then, the estimate (4.31) directly follows from (4.26) and (4.27). \square

Thanks to Proposition 8 above, to finish the proof of Theorem 1, it suffices to study the spectral gap of $\mathcal{L}_{\text{local}}$ on the syndrome space $\mathcal{B}_{1,1}$, i.e., step (c) outlined in Section 3. This is the goal of the next section.

4.2.1 Analysis of the quasi-1D structure

In this section, we will analyze the spectral gap of the local Davies generator $\mathcal{L}_{\text{local}}$ in the syndrome space. The main result is stated as follows.

Proposition 9. *Let $\mathcal{L}_{\text{local}}$ be defined in (4.13) and $\mathcal{B}_{1,1}$ be defined in Corollary 7, we have*

$$\text{Gap}(-\mathcal{L}_{\text{local}}|_{\mathcal{B}_{1,1}}) = \max\left\{e^{-\mathcal{O}(\beta)}, \Omega(N^{-3})\right\}.$$

Then, Theorem 1 is a corollary of Proposition 8 and Proposition 9. To prove the above proposition, we consider

$$\mathcal{L}_1 := \sum_{j \in \text{snake}} \mathcal{L}_{\sigma_j^x}, \quad \mathcal{L}_2 := \sum_{j \in \text{comb}} \mathcal{L}_{\sigma_j^z}. \quad (4.32)$$

From Lemma 6, it is straightforward to see that \mathcal{L}_1 and \mathcal{L}_2 commutes and only act nontrivially on $\mathcal{A}_{\text{m}}^{\text{full}}$ and $\mathcal{A}_{\text{e}}^{\text{full}}$, respectively. Thus, we can analyze the spectral gap of \mathcal{L}_1 and \mathcal{L}_2 separately. Proposition 9 directly follows from the following two lemmas.

Lemma 10. *Let $\mathcal{A}_{\text{m}}^{\text{full}}$ be defined as in Lemma 5, we have*

$$\text{Gap}(-\mathcal{L}_1|_{\mathcal{A}_{\text{m}}^{\text{full}}}) = \max\left\{e^{-\mathcal{O}(\beta)}, \Omega(N^{-3})\right\}. \quad (4.33)$$

Lemma 11. *Let $\mathcal{A}_e^{\text{full}}$ be defined as in Lemma 5, we have*

$$\text{Gap} \left(-\mathcal{L}_2|_{\mathcal{A}_e^{\text{full}}} \right) = \max \left\{ e^{-\mathcal{O}(\beta)}, \Omega(N^{-2.5}) \right\}.$$

The $\exp(-\mathcal{O}(\beta))$ spectral gap of $\text{Gap}(-\mathcal{L}_1|_{\mathcal{A}_m^{\text{full}}})$ and $\text{Gap}(-\mathcal{L}_2|_{\mathcal{A}_e^{\text{full}}})$ has been proved in [AFH09, Section 7]. In what follows, we focus on the gap estimate of order $\text{poly}(N^{-1})$. We first prove Lemma 10.

Proof of Lemma 10. Recall that $\mathcal{A}_m^{\text{full}} = \mathcal{B}(\mathcal{H}_b^m)$ is spanned by the basis matrices $|m\rangle\langle m'|$, where $m, m' \in \{-1, 1\}^{L^2}$ and $\#\{m_i = -1\}, \#\{m'_i = -1\} \in 2\mathbb{Z}$. We note that this set of basis matrices $\{|m\rangle\langle m'|\}$ also forms an orthogonal basis for $\mathcal{A}_m^{\text{full}}$ with respect to the GNS inner product defined as in (2.8) by the reduced Gibbs state $\text{Tr}_{\mathcal{A}_e^{\text{full}}}(\sigma_\beta) \propto \exp(-\beta \sum_p \mathbf{Z}_p)$ ¹.

We next decompose the space $\mathcal{A}_m^{\text{full}}$ such that \mathcal{L}_1 presents a block diagonal form. Note that $\mathcal{A}_m^{\text{full}}$ is spanned by $|m'\rangle\langle m|$ with $|m\rangle, |m'\rangle \in \mathcal{H}_b^m$ having an even number of $-$ signs. For any $\Lambda \subset \{1, 2, \dots, L^2\}$ with even $L^2 - |\Lambda|$, we introduce the subspace $\mathcal{A}_m^{\text{full}}(\Lambda)$ of $\mathcal{A}_m^{\text{full}}$ spanned by $|m'\rangle\langle m|$, where $m = m'$ on Λ and $m = -m'$ on the complement $\Lambda^c := \{1, 2, \dots, L^2\} \setminus \Lambda$. It is straightforward to check that the subspaces $\mathcal{A}_m^{\text{full}}(\Lambda)$ are orthogonal with respect to both the GNS and HS inner products, and thereby

$$\mathcal{A}_m^{\text{full}} = \bigoplus_{\substack{\Lambda \subset \{1, \dots, L^2\}: \\ L^2 - \Lambda \text{ even}}} \mathcal{A}_m^{\text{full}}(\Lambda). \quad (4.34)$$

In addition, by writing $|m'\rangle\langle m| = (|m\rangle\langle m|)_\Lambda \otimes (|-m\rangle\langle m|)_{\Lambda^c} \in \mathcal{A}_m^{\text{full}}(\Lambda)$, we can further decompose

$$\mathcal{A}_m^{\text{full}}(\Lambda) = \mathcal{A}^{\text{ab}}(\Lambda) \otimes \mathcal{F}(\Lambda),$$

where $\mathcal{A}^{\text{ab}}(\Lambda)$ is the Abelian algebra generated by the projections on bonds restricted to Λ and $\mathcal{F}(\Lambda)$ is the space spanned by flips of bonds restricted to Λ^c . We observe that any partition of $\{1, 2, \dots, L^2\}$ into $\Lambda \cup \Lambda^c$ induces a partition of the spins j on the snake, equivalently, pairs of neighboring plaquettes/bonds $\{\mathbf{Z}_{j-1}, \mathbf{Z}_j\}$ into three sets: Γ_{flip} for both bonds in Λ^c , Γ_{ab} for both bonds in Λ , and Γ_{int} for one bond in Λ and the other in Λ^c .

The following lemma extends [AFH09, Lemma 5], which was originally stated for the 1D ferromagnetic Ising model. We provide a self-contained proof in Section 4.3 with explicit computations of the local matrix representations of the master Hamiltonian of \mathcal{L}_1 .

Lemma 12. *\mathcal{L}_1 , defined in (4.32), on $\mathcal{A}_m^{\text{full}}$ is block diagonal for the decomposition (4.34).*

Now, we are ready to estimate the gap of \mathcal{L}_1 on each $\mathcal{A}_m^{\text{full}}(\Lambda)$ by the following three cases.

- If $\Gamma_{\text{int}} \neq \emptyset$, by Eq. (4.54) in the proof of Lemma 12, under an orthonormal basis with respect to the GNS inner product, the master Hamiltonian of $-\mathcal{L}_{\sigma_j^x}$ on $\mathcal{A}_m^{\text{full}}(\Lambda)$ takes the form:

$$I_{j-2} \otimes \begin{bmatrix} \frac{h_-+1}{2} & 0 & 0 & 0 \\ 0 & \frac{h_++1}{2} & 0 & 0 \\ 0 & 0 & \frac{h_-+1}{2} & 0 \\ 0 & 0 & 0 & \frac{h_++1}{2} \end{bmatrix} \otimes I_{L^2-j} \succeq \frac{1}{2}. \quad (4.35)$$

¹Note from Lemma 5 that $\sigma_\beta \in \mathcal{A}_m^{\text{full}} \otimes \mathcal{A}_e^{\text{full}}$.

This implies

$$-\left\langle A, \mathcal{L}_1|_{\mathcal{A}_m^{\text{full}}(\Lambda)} A \right\rangle_{\sigma_\beta} \geq \sum_{j \in \Gamma_{\text{int}}} -\left\langle A, \mathcal{L}_{\sigma_j^x}|_{\mathcal{A}_m^{\text{full}}(\Lambda)} A \right\rangle_{\sigma_\beta} \geq |\Gamma_{\text{int}}| \cdot \frac{1}{2} \langle A, A \rangle_{\sigma_\beta}.$$

for any $A \in \mathcal{A}_m^{\text{full}}(\Lambda)$, where the first step is by $-\mathcal{L}_{\sigma_j^x} \succeq 0$. It follows that

$$-\mathcal{L}_1|_{\mathcal{A}_m^{\text{full}}(\Lambda)} \succeq \frac{|\Gamma_{\text{int}}|}{2}. \quad (4.36)$$

- If $\Gamma_{\text{flip}} = \{1, 2, \dots, L^2\}$ (i.e., $\Lambda = \emptyset$), by (4.53), the master Hamiltonian of $-\mathcal{L}_{\sigma_j^x}$ on $\mathcal{A}_m^{\text{full}}(\emptyset)$ is

$$I_{j-2} \otimes \begin{bmatrix} -\frac{h_++h_-}{2} & 0 & 0 & 0 \\ 0 & -1 & 1 & 0 \\ 0 & 1 & -1 & 0 \\ 0 & 0 & 0 & -\frac{h_++h_-}{2} \end{bmatrix} \otimes I_{L^2-j}. \quad (4.37)$$

This case has already been discussed in [AFH09] (see after Proposition 2), from which we have

$$-\mathcal{L}_1|_{\mathcal{A}_m^{\text{full}}(\emptyset)} \succeq \frac{1}{2}. \quad (4.38)$$

- If $\Gamma_{\text{ab}} = \{1, 2, \dots, L^2\}$ (i.e., $\Lambda = [L^2]$), [AFH09, Proposition 2] has given a spectral gap lower bound that exponentially decays in β . However, this lower bound is far from sharp at low temperature. Next, we shall derive a lower bound of gap polynomially decaying in N but independent of β , which is summarized in the following lemma.

Lemma 13. *Given the notation above, we have, when $\beta = \Omega(\ln N)$,*

$$\text{Gap} \left(-\mathcal{L}_1|_{\mathcal{A}_m^{\text{full}}([L^2])} \right) = \Omega(N^{-3}).$$

Once Lemma 13 is proved, we can combine it with Lemma 12, as well as (4.36) and (4.38), to obtain the desired (4.33):

$$\text{Gap} \left(-\mathcal{L}_1|_{\mathcal{A}_m^{\text{full}}} \right) \geq \min \left\{ \frac{1}{2}, \text{Gap} \left(-\mathcal{L}_1|_{\mathcal{A}_m^{\text{full}}([L^2])} \right) \right\} = \Omega(N^{-3}).$$

We next prove Lemma 13 to conclude the proof of Lemma 10. From (4.52), the matrix representation of the master Hamiltonian of $-\mathcal{L}_1$ can be written as:

$$K_{L^2}^\beta = K_{L^2} + (K_{L^2}^\beta - K_{L^2}),$$

where K_{L^2} is the matrix representation at zero temperature (i.e., $\beta \rightarrow \infty$):

$$K_{L^2} = \underbrace{\sum_{i=0}^{L^2-2} I_i \otimes k_T \otimes I_{L^2-2-i}}_{:=K_T} + \underbrace{\sum_{i=0}^{L^2-2} I_i \otimes k_D \otimes I_{L^2-2-i}}_{:=K_D}, \quad (4.39)$$

with

$$k_T = \begin{bmatrix} 0 & 0 & 0 & 0 \\ 0 & 1 & -1 & 0 \\ 0 & -1 & 1 & 0 \\ 0 & 0 & 0 & 0 \end{bmatrix}, \quad k_D = \begin{bmatrix} 0 & 0 & 0 & 0 \\ 0 & 0 & 0 & 0 \\ 0 & 0 & 0 & 0 \\ 0 & 0 & 0 & 2 \end{bmatrix}. \quad (4.40)$$

and $K_{L^2}^\beta - K_{L^2}$ is given by

$$K_{L^2}^\beta - K_{L^2} = \sum_{i=0}^{N-2} I_i \otimes \begin{bmatrix} \frac{2\eta^2}{\eta^2+1} & 0 & 0 & -\frac{2\eta}{\eta^2+1} \\ 0 & 0 & 0 & 0 \\ 0 & 0 & 0 & 0 \\ -\frac{2\eta}{\eta^2+1} & 0 & 0 & -\frac{2\eta^2}{\eta^2+1} \end{bmatrix} \otimes I_{L^2-2-i},$$

where $\eta = \exp(-2\beta)$. The operator norm of the self-adjoint operator $K_{L^2}^\beta - K_{L^2}$ can be directly estimated as

$$\|K_{L^2}^\beta - K_{L^2}\| = \Theta(L^2 e^{-2\beta}) = \mathcal{O}(L^{-8}), \quad \text{when } \beta \geq 5 \ln L.$$

Therefore, to obtain the desired gap estimate (A.9), we only need to consider the gap at zero temperature and prove $\text{Gap}(K_{L^2}) \geq \Omega(L^{-6})$.

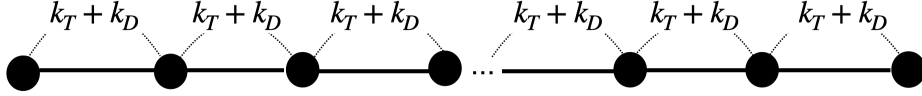


Figure 4: Action of \mathcal{L}_1 ($\beta \rightarrow \infty$) on Γ_{ab} . k_T and k_D are defined in (4.40). Each black dot represents a bond corresponding to the plaquette observable \mathbf{Z}_j ordered by the snake.

For this, we consider the following configuration space

$$\mathcal{S}_{L^2} = \text{Span}(\mathcal{A}_{L^2}) \cong \mathbb{C}^{2^{L^2}}, \quad \text{with } \mathcal{A}_{L^2} = \{+, -\}^{\otimes L^2}, \quad (4.41)$$

with the space decomposition $\mathcal{S}_{L^2} = \bigoplus_k \mathcal{S}_{L^2,k}$, where $\mathcal{S}_{L^2,k} = \text{Span}(\mathcal{A}_{L^2,k})$ with

$$\mathcal{A}_{L^2,k} := \left\{ a \in \{+, -\}^{\otimes L^2} \mid a \text{ has } k \text{ “-” signs} \right\}.$$

It is clear from the construction that the action of $-\mathcal{L}_1$ on $\mathcal{A}_{\text{m}}^{\text{full}}(\Lambda)$ with $\Lambda = \Gamma_{\text{ab}} = \{1, 2, \dots\}$ is the same as the action of $K_{L^2}^\beta$ on $\bigoplus_{k \text{ even}} \mathcal{S}_{L^2,k}$ under the identification $|m\rangle \langle m| \rightarrow |m\rangle$. One can also readily check that

$$K_{L^2} : \mathcal{S}_{L^2,k} \rightarrow \mathcal{S}_{L^2,k}, \quad (4.42)$$

that is, K_{L^2} is block diagonal for the decomposition $\mathcal{S}_{L^2} = \bigoplus_k \mathcal{S}_{L^2,k}$.

When $k = 0$, we have $K_{L^2}|_{\mathcal{A}_{L^2,0}} = 0$ and $\dim(\mathcal{A}_{L^2,0}) = 1$. Thus,

$$\text{Gap}(-\mathcal{L}_1|_{\mathcal{A}_{\text{m}}^{\text{full}}([L^2])}) \geq \min_{k=2,3,4,\dots} \lambda_{\min}(K_{L^2}|_{\mathcal{S}_{L^2,k}}).$$

In principle, we only need to consider the admissible configuration, that is, the subspaces $\mathcal{S}_{L^2,k}$ with even k . However, it is simpler to prove a result for all k 's via iterative reduction. We emphasize that such a relaxation does not produce any additional dependence on the system size $N = 2L^2$, and hence will not give a worse spectral gap lower bound.

We now consider the lower bound of K_{L^2} on each $\mathcal{S}_{L^2,k}$ for $k > 0$. Define

$$\lambda_{L^2,k} := \lambda_{\min} \left(K_{L^2}|_{\mathcal{S}_{L^2,k}} \right).$$

We first note that when $k = L^2$, it also holds that $\dim(\mathcal{S}_{L^2,L^2}) = 1$, and

$$K_{L^2}|_{\mathcal{S}_{L^2,L^2}} = K_D|_{\mathcal{S}_{L^2,L^2}} \succeq 2(L^2 - 1) \geq 1.$$

When $k \geq 3$ and $L^2 \geq 3$, we use the following iteration to reduce the estimation of $\lambda_{L^2,k}$ to $\lambda_{L^2,2}$. By the representation (4.39) of K_{L^2} , we find

$$K_{L^2} = K_{L^2-1} \otimes I_1 + I_{L^2-2} \otimes (k_T + k_D).$$

In addition, there holds

$$\mathcal{S}_{L^2,k} = \text{Span}(\mathcal{A}_{L^2-1,k} \otimes |+\rangle) \oplus \text{Span}(\mathcal{A}_{L^2-1,k-1} \otimes |-\rangle).$$

Thus, for any given $a = a_+ \otimes |+\rangle + a_- \otimes |-\rangle \in \mathcal{S}_{L^2,k}$ with $|a_+|^2 + |a_-|^2 = 1$, we can derive

$$\begin{aligned} a^* K_{L^2} a &\geq a^* (K_{L^2-1} \otimes I_1) a \\ &= (a_+)^* K_{L^2-1} a_+ + (a_-)^* K_{L^2-1} a_- \\ &\geq \min \{ \lambda_{L^2-1,k}, \lambda_{L^2-1,k-1} \}, \end{aligned} \tag{4.43}$$

where the first inequality follows from $k_T + k_D \succeq 0$, the second inequality follows from (4.42) and $a_+ \in \mathcal{S}_{L^2-1,k}$, $a_- \in \mathcal{S}_{L^2-1,k-1}$.

Therefore, it suffices to estimate $\lambda_{L^2,2}$ to finish. To do so, we find, by (4.39),

$$K_{L^2}|_{\mathcal{A}_{L^2,2}} = (K_T)|_{\mathcal{A}_{L^2,2}} + (K_D)|_{\mathcal{A}_{L^2,2}},$$

and $K_T(\varphi) = 0$ for $\varphi \in \mathcal{A}_{L^2,2}$ if and only if $I_i \otimes k_T \otimes I_{L^2-2-i}(\varphi) = 0$ for all i , which implies

$$\text{Ker} \left(K_T|_{\mathcal{A}_{L^2,2}} \right) = \text{Span} \left\{ \sum_{a \in \mathcal{A}_{L^2,2}} a \right\}.$$

Then, it follows that

$$\begin{aligned} &\left(\sqrt{\frac{2}{L^2(L^2-1)}} \sum_{a \in \mathcal{A}_{L^2,2}} a \right)^* K_D \left(\sqrt{\frac{2}{L^2(L^2-1)}} \sum_{a \in \mathcal{A}_{L^2,2}} a \right) \\ &= \frac{4}{L^2(L^2-1)} \left(\sum_{a \in \mathcal{A}_{L^2,2}^-} a \right)^* \left(\sum_{a \in \mathcal{A}_{L^2,2}^-} a \right) = \frac{4}{L^2}, \end{aligned}$$

where $\mathcal{A}_{L^2,2}^{--} := \left\{ a \in \{+, -\}^{\otimes L^2} \mid a \text{ has 2 consecutive " - " signs} \right\}$. By Lemma 3 (item 4) and $\|K_D|_{\mathcal{A}_{L^2,2}}\| = \mathcal{O}(1)$, we have

$$K_T|_{\mathcal{A}_{L^2,2}} + K_D|_{\mathcal{A}_{L^2,2}} \succeq \frac{(4/L^2)\text{Gap}\left(K_T|_{\mathcal{A}_{L^2,2}}\right)}{\text{Gap}\left(K_T|_{\mathcal{A}_{L^2,2}}\right) + \mathcal{O}(1)}. \quad (4.44)$$

We next estimate the spectral gap of $(K_T)|_{\mathcal{A}_{L^2,2}}$. We note from (4.39)-(4.40) that K_T can be identified as a ferromagnetic Heisenberg-1/2 model on L^2 particles:

$$K_T = -\frac{1}{2} \sum_{j=1}^{L^2-1} \left(\sigma_j^x \sigma_{j+1}^x + \sigma_j^y \sigma_{j+1}^y + \sigma_j^z \sigma_{j+1}^z - I \right).$$

From [KN97, Proposition 2] for the Heisenberg model, we have

$$\text{Gap}\left((K_T)|_{\mathcal{A}_{L^2,2}}\right) \geq \text{Gap}(K_T) = \Omega(L^{-4}).$$

Plugging this back into (4.44), we have

$$\lambda_{L^2,2} = \Omega(L^{-6}). \quad (4.45)$$

Using Eq. (4.43), it follows that $\min_{3 \leq k \leq L^2} \lambda_{L^2,k} = \Omega(L^{-6})$ and $\text{Gap}\left(-\mathcal{L}_1|_{\mathcal{A}_{\text{m}}^{\text{full}}([L^2])}\right) = \Omega(L^{-6})$. To summarize, there holds

$$\text{Gap}(-\mathcal{L}_1) \geq \min\left\{\frac{1}{2}, \text{Gap}\left(-\mathcal{L}_1|_{\mathcal{A}_{\text{m}}^{\text{full}}([L^2])}\right)\right\} = \Omega(L^{-6}) = \Omega(N^{-3}), \quad (4.46)$$

for $\beta \geq 5 \ln L$. This concludes the proof of Lemma 13, and consequently Lemma 10. \square

We next prove Lemma 11, whose basic ideas are similar to that of Lemma 10 but require some more technical arguments due to the comb structure. To be specific, recall the formula (4.18), the local master Hamiltonian representation of $\mathcal{L}_{\sigma_j^z}$ is the same as that of $\mathcal{L}_{\sigma_j^x}$. However, here \mathcal{L}_1 acts on a 1D straight line (snake), where each observable \mathbf{Z}_p connects only two neighboring qubits along the chain, while \mathcal{L}_2 acts on a comb-like 1D structure, where some observables \mathbf{X}_s can connect three neighboring qubits on the comb. This difference prevents us from directly applying the proof of Lemma 10.

Proof of Lemma 11. The starting point of the proof of Lemma 11 follows from that of Lemma 10. We recall that $\mathcal{A}_{\text{e}}^{\text{full}}$ is spanned by the orthogonal basis $|e'\rangle \langle e|$ for the GNS inner product induced by the reduced Gibbs state $\text{Tr}_{\mathcal{A}_{\text{m}}^{\text{full}}}(\sigma_\beta) \propto \exp(-\beta \sum_s \mathbf{X}_s)$, where $e, e' \in \{+, -\}^{L^2}$ and $\# \{e_i = -1\}, \# \{e'_i = -1\} \in 2\mathbb{Z}$. Moreover, we decompose $\mathcal{A}_{\text{e}}^{\text{full}} = \bigoplus_{\Lambda} \mathcal{A}_{\text{e}}^{\text{full}}(\Lambda)$, where $\Lambda \subset \{1, 2, \dots, L^2\}$ with even $L^2 - |\Lambda|$ and the subspace $\mathcal{A}_{\text{e}}^{\text{full}}(\Lambda)$ is spanned by $|e'\rangle \langle e|$, where $e = e'$ on Λ and $e = -e'$ on $\{1, 2, \dots, L^2\} \setminus \Lambda$. We also partition pairs of neighboring bonds into three sets: Γ_{flip} for both bonds in Λ^c , Γ_{ab} for both bonds in Λ , and Γ_{int} for one bond in Λ and the other in Λ^c .

Then, a similar lemma as Lemma 12 holds for \mathcal{L}_2 , since its proof only needs the properties of local Lindbladians $\mathcal{L}_{\sigma_j^z}$ that are the same as those of $\mathcal{L}_{\sigma_j^x}$.

Lemma 14. \mathcal{L}_2 , defined in (4.32), on $\mathcal{A}_e^{\text{full}}$ is block diagonal for the decomposition:

$$\mathcal{A}_e^{\text{full}} = \bigoplus_{\substack{\Lambda \subset \{1, \dots, L^2\}: \\ L^2 - \Lambda \text{ even}}} \mathcal{A}_e^{\text{full}}(\Lambda).$$

Next, we consider three cases: 1. $\Gamma_{\text{int}} \neq \emptyset$; 2. $\Gamma_{\text{flip}} = \{1, \dots, L^2\} := [L^2]$; 3. $\Gamma_{\text{ab}} = [L^2]$. Noting that again, the arguments of (4.36) and (4.38) only uses local Lindbladians $\mathcal{L}_{\sigma_j^x}$, we have similar estimates for \mathcal{L}_2 :

$$-\mathcal{L}_2|_{\mathcal{A}_e^{\text{full}}(\Lambda), \Gamma_{\text{int}} \neq \emptyset} \succeq \frac{1}{2} \quad \text{and} \quad -\mathcal{L}_2|_{\mathcal{A}_e^{\text{full}}(\emptyset)} \succeq \frac{1}{2}.$$

We now consider the third case $\Gamma_{\text{ab}} = [L^2]$ and prove the following result, which finishes the proof of Lemma 11.

Lemma 15. *Given the notation above, we have, when $\beta = \Omega(\ln N)$,*

$$\text{Gap} \left(-\mathcal{L}_2|_{\mathcal{A}_m^{\text{full}}([L^2])} \right) = \Omega(N^{-2.5}).$$

Following the notation in the proof of Lemma 13, we still consider the subspace \mathcal{S}_{L^2} in (4.41) and denote by $K_{L^2}^\beta$ the matrix representation of the master Hamiltonian of $-\mathcal{L}_2$. Moreover, we similarly have

$$\left\| K_{L^2}^\beta - K_{L^2} \right\| = \Theta(L^2 e^{-2\beta}) = \mathcal{O}(L^{-8}), \quad \text{for } \beta \geq 5 \ln L,$$

where $K_{L^2} := K_{L^2}^\infty$. One can also see that each local term in K_{L^2} has the same form as the one in (4.40), but the tensor structure is different²; see Fig. 5. We then decompose \mathcal{S}_{L^2} according to number of “ $-$ ” signs in the entry of basis:

$$\mathcal{S}_{L^2} = \bigoplus_k \mathcal{S}_{L^2, k}, \quad \mathcal{S}_{L^2, k} = \text{Span}(\mathcal{A}_{L^2, k}), \quad (4.47)$$

with

$$\mathcal{A}_{L^2, k} := \left\{ a \in \{+, -\}^{\otimes L^2} \mid a \text{ has } k \text{ “} - \text{” signs} \right\}.$$

Then, K_{L^2} is block diagonal for (4.47) and

$$\text{Gap}(K_{L^2}) \geq \min_{k=2,3,4,\dots} \lambda_{\min} \left(K_{L^2}|_{\mathcal{S}_{L^2, k}} \right).$$

We first consider the subspace $\mathcal{S}_{L^2, 2}$, whose basis vectors contain only two “ $-$ ” signs. Our strategy for lower bounding $\lambda_{\min} \left(K_{L^2}|_{\mathcal{S}_{L^2, 2}} \right)$ is to reduce this problem to a straight line case as in Fig. 4. For this, we introduce a set of lines that covering all vertices in the comb. More specifically, we may regard the comb as a connected graph (more precisely, a tree) with L^2 vertices of degree at most 3, each corresponding to a star \mathbf{X}_s that interacts the comb. Let

²Since the qubits and star observables on the comb cannot be ordered along a line, some local term in K_{L^2} is of the form $I \otimes a \otimes I \otimes b \otimes I$ with a, b being non-identity 2×2 matrix. Since some observable \mathbf{X}_s is altered by three $\mathcal{L}_{\sigma_j^z}$, there are some sites where we find three local terms in K_{L^2} nontrivially acting on it.

\mathbf{D}_{comb} be the set of degree-one vertices (i.e., end-points) in the comb, and $l_{u,v}$ be the shortest path between the vertices u and v in the comb. Define

$$\mathbf{P}_{\text{comb}} := \{l_{u,v} : \forall u \neq v \in \mathbf{D}_{\text{comb}}\}. \quad (4.48)$$

Then, we know that \mathbf{P}_{comb} contains $L(L-1)/2 = \mathcal{O}(L^2)$ (simple) paths, and the maximum length of the paths is $\ell_{\text{comb}} = 3L - 2$. Two examples of these paths are given in Fig. 6.

For an arbitrary unit vector $\alpha \in \mathcal{S}_{L^2,2}$:

$$\alpha = \sum_{a \in \mathcal{A}_{L^2,2}} p_a |a\rangle ,$$

by Fact 16, there exists a path \tilde{l} in \mathbf{P}_{comb} such that for

$$\alpha_{\tilde{l}} := \sum_{a \in \mathcal{A}_{L^2,k} : \#\{s \in \tilde{l} : a_s = "-" \} > 1} p_a |a\rangle ,$$

it holds that

$$\|\alpha_{\tilde{l}}\|_2^2 = \Omega(1/L^2). \quad (4.49)$$

Let $(K_{L^2})_{\tilde{l}}$ be the restriction of K_{L^2} to the path \tilde{l} . More specifically,

$$(K_{L^2})_{\tilde{l}} := \sum_{e=(u,v) \in \tilde{l}} (k_T + k_D)_{u,v} ,$$

where $(k_T + k_D)_{u,v}$ is a local term that applies $k_T + k_D$ to the “qubits” at u and v . Then, we have

$$\begin{aligned} \alpha^* K_{L^2} \alpha &\geq \alpha^* (K_{L^2})_{\tilde{l}} \alpha \\ &\geq \alpha_{\tilde{l}}^* (K_{L^2})_{\tilde{l}} \alpha_{\tilde{l}} \\ &\geq \|\alpha_{\tilde{l}}\|_2^2 \cdot \lambda_{\ell_{\text{comb}},2} \\ &= \Omega(L^{-2}) \cdot \Omega(L^{-3}) = \Omega(L^{-5}), \end{aligned} \quad (4.50)$$

where the first step follows from $K_{L^2} - (K_{L^2})_{\tilde{l}}$ is positive semi-definite, the second step follows from $\langle \alpha - \alpha_{\tilde{l}}, (K_{L^2})_{\tilde{l}} \alpha_{\tilde{l}} \rangle = 0$, the third step follows from $(K_{L^2})_{\tilde{l}}$ is equivalent to a 1D chain of length $|\tilde{l}| \leq \ell_{\text{comb}} = \mathcal{O}(L)$ and $a_{\tilde{l}} \in \mathcal{S}_{|\tilde{l}|,2}$, and the last step follows from (4.49) and (4.45).

Thus, we conclude

$$K_{L^2}|_{\mathcal{S}_{L^2,2}} = \Omega(L^{-5}) = \Omega(N^{-2.5}).$$

We proceed to estimate $\lambda_{\min}(K_{L^2}|_{\mathcal{S}_{L^2,k}})$ for $k \geq 3$. For an arbitrary unit vector $\alpha \in \mathcal{S}_{L^2,k}$:

$$\alpha = \sum_{a \in \mathcal{A}_{L^2,k}} p_a |a\rangle ,$$

by Fact 16, there exists a path \tilde{l} in \mathbf{P}_{comb} such that for

$$\alpha_{\tilde{l},q} := \sum_{\substack{a \in \mathcal{A}_{L^2,k} : \\ \#\{s \in \tilde{l} : a_s = "-" \} = q}} p_a |a\rangle \quad \forall 2 \leq q \leq k ,$$

we have

$$\sum_{q=2}^k \|\alpha_{\tilde{l},q}\|_2^2 = \Omega(1/L^2). \quad (4.51)$$

Let $(K_{L^2})_{\tilde{l}}$ be the restriction of K_{L^2} to the path \tilde{l} . Then, we find, similar to (4.50),

$$\begin{aligned} \alpha^* K_{L^2} \alpha &\geq \alpha^* (K_{L^2})_{\tilde{l}} \alpha \\ &\geq \sum_{q=2}^k \alpha_{\tilde{l},q}^* (K_{L^2})_{\tilde{l}} \alpha_{\tilde{l},q} \\ &\geq \sum_{q=2}^k \|\alpha_{\tilde{l},q}\|_2^2 \cdot \lambda_{\ell_{\text{comb}},q} \\ &\geq \sum_{q=2}^k \|\alpha_{\tilde{l},q}\|_2^2 \cdot \lambda_{\ell_{\text{comb}},2} \\ &= \Omega(L^{-2}) \cdot \Omega(L^{-3}) = \Omega(L^{-5}), \end{aligned}$$

where the first step follows from $K_{L^2} - (K_{L^2})_{\tilde{l}}$ is positive semi-definite, the second step follows from $\alpha_{\tilde{l},q_1}^* (K_{L^2})_{\tilde{l}} \alpha_{\tilde{l},q_2} = 0$ for $q_1 \neq q_2$, the third step follows from $(K_{L^2})_{\tilde{l}}$ is equivalent to a 1D chain of length $|\tilde{l}| \leq \ell_{\text{comb}} = O(L)$, and $\alpha_{\tilde{l},q}$ is in the subspace $\mathcal{S}_{|\tilde{l}|,q}$, the fourth step follows from the recursion relation (4.43) that $\lambda_{\ell_{\text{comb}},q} \geq \lambda_{\ell_{\text{comb}},2}$, and the last step follow from (4.45) and (4.51). Thus, we have

$$K_{L^2}|_{\mathcal{S}_{L^2,k}} = \Omega(L^{-5}) = \Omega(N^{-2.5}).$$

Combining them all together, we now can conclude

$$\text{Gap} \left(-\mathcal{L}_2|_{\mathcal{A}_e^{\text{full}}([L^2])} \right) \geq \min_{2 \leq k \leq L^2} \lambda_{\min} \left(K_{L^2}|_{\mathcal{S}_{L^2,k}} \right) - \mathcal{O}(N^{-4}) = \Omega(N^{-2.5}).$$

This concludes the proof of Lemma 15, and thus the proof of Lemma 11. \square

Fact 16. *Let $2 \leq k \leq L^2 - 1$. For any unit vector $\alpha \in \mathcal{S}_{L^2,k}$ of the form:*

$$\alpha = \sum_{a \in \mathcal{A}_{L^2,k}} p_a |a\rangle,$$

there exists a path $\tilde{l} \in \mathbf{P}_{\text{comb}}$ defined as (4.48) such that

$$\sum_{\substack{a \in \mathcal{A}_{L^2,k}: \\ \#\{s \in \tilde{l}: a_s = "-" \} > 1}} |p_a|^2 = \Omega(1/L).$$

Proof. We first observe that for any $a \in \{+, -\}^{L^2}$ with k “-”, by the construction of \mathbf{P}_{comb} , there exists at least one path $l \in \mathbf{P}_{\text{comb}}$ that contains at last two “-” on it. Then, we have

$$\begin{aligned} \sum_{l \in \mathbf{P}_{\text{comb}}} \sum_{\substack{a \in \mathcal{A}_{L^2, k}: \\ \#\{s \in l: a_s = \text{“-”}\} > 1}} |p_a|^2 &= \sum_{a \in \mathcal{A}_{L^2, k}} |p_a|^2 \cdot \#\{l \in \mathbf{P}_{\text{comb}} : \#\{s \in l : a_s = \text{“-”}\} > 1\} \\ &\geq \sum_{a \in \mathcal{A}_{L^2, k}} |p_a|^2 \cdot 1 \\ &= 1, \end{aligned}$$

where the first step follows from exchanging the summations, the second step follows from our observation, and the last step follows from α is a unit vector. Since \mathbf{P}_{comb} contains L^2 paths, by the averaging argument, there must exists an $\tilde{l} \in \mathbf{P}_{\text{comb}}$ such that

$$\sum_{\substack{a \in \mathcal{A}_{L^2, k}: \\ \#\{s \in \tilde{l}: a_s = \text{“-”}\} > 1}} |p_a|^2 \geq 1/L,$$

which proves the proposition. \square

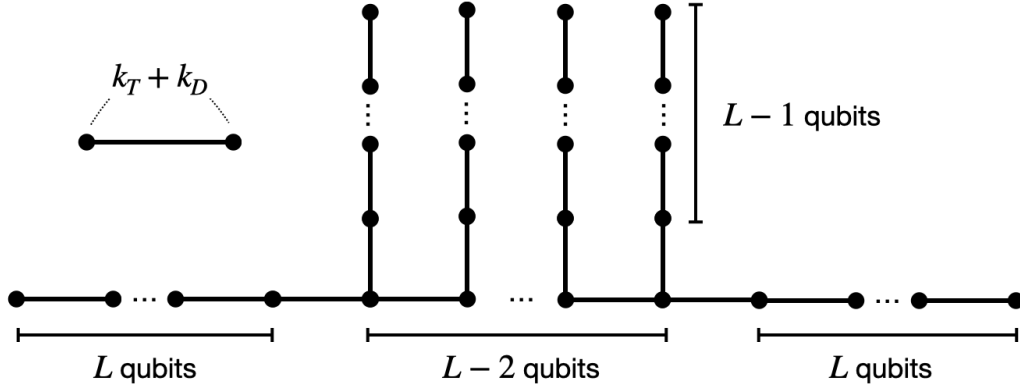


Figure 5: The underlying graph of $\sum_{j \in \text{comb}} \mathcal{L}_{\sigma_j^z}$ acting on $\mathcal{A}_e^{\text{full}}$. Here, each black dot represents a qubit corresponding to a bond observation of \mathbf{X}_{s_j} . The transition matrix $k_T + k_D$ induced by $\mathcal{L}_{\sigma_j^z}$ acts on each neighboring qubits.

4.3 Proof of Lemmas

We collect proofs of some technical lemmas for the spectral gap analysis.

Proof of Lemma 5. The decomposition (4.11) is straightforward by the construction. Here we only prove the fact that the algebra $\mathcal{A}_m^{\text{full}} = \mathcal{B}(\mathcal{H}_b^m)$ can be generated by $\{\mathbf{Z}_p\}_p \cup \{\sigma_j^x\}_{j \in \text{snake}}$. The claim for $\mathcal{A}_e^{\text{full}}$ can be similarly proved. Indeed, each basis (admissible bond) $|m\rangle$ in \mathcal{H}_b^m can be identified as a Pauli string $\sigma_{j_1}^x \cdots \sigma_{j_k}^x$ with j_i on the snake. Each operator on \mathcal{H}_b^m can be written as the linear combination of $|m'\rangle \langle m|$, where $|m\rangle$ and $|m'\rangle$ are admissible bonds.

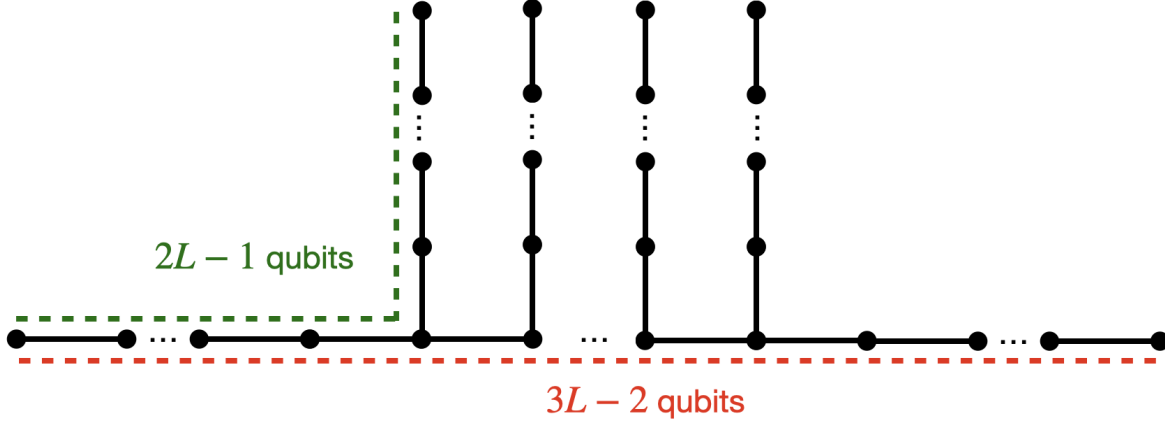


Figure 6: Examples of lines on the graph.

Meanwhile, each $|m'\rangle\langle m|$ with $|m'\rangle \neq |m\rangle$ is a composition of flips of neighboring states. Thus, it suffices to consider the case $|m'\rangle\langle m|$ that maps the state $|m\rangle = \sigma_{j_1}^x \cdots \sigma_{j_k}^x | +1^{L^2} \rangle^3$ to a neighboring one $|m'\rangle = \sigma_{j_2}^x \cdots \sigma_{j_k}^x | +1^{L^2} \rangle$, which can be easily constructed using $\{\mathbf{Z}_p\}_p$ and $\{\sigma_j^x\}_{j \in \text{snake}}$. Here we give the representation for $|m'\rangle\langle m|$:

$$|m'\rangle\langle m| = \underbrace{\frac{I - m_{j_1} \mathbf{Z}_{j_1}}{2}}_{|m\rangle \rightarrow 0, |m'\rangle \rightarrow |m'\rangle} \cdot \underbrace{\left(\prod_{j \neq j_1-1, j_1}^{L^2} \frac{I + m_j \mathbf{Z}_j}{2} \right) \sigma_{j_1}^x}_{=|m'\rangle\langle m| + |m\rangle\langle m'|}.$$

The case of $|m\rangle\langle m|$ can be similarly done. \square

Proof of Lemma 6. The formula (4.22) follows from the representation of \mathcal{L}_O with $O = X_1, X_2, Z_1, Z_2$ and the fact from (5) that these global jumps commute with the algebras $\mathcal{A}_{m/e}^{\text{full}}$. For the formula (4.22), it suffices to note that $\{\sigma_j^x\}_{j \in \text{snake}}$ and the projections (4.14) belong to $\mathcal{A}_m^{\text{full}}$ and commute with $\mathcal{Q}_1 \otimes \mathcal{Q}_2 \otimes \mathcal{A}_e^{\text{full}}$. The formula (4.23) follows from the same reason by the computation (4.18). The first two statements of (4.24) can be proved by a very similar argument as [AFH09, Lemma 6]. To show $\text{Ker}(\mathcal{L}_{\text{global}}) = \mathbf{1} \otimes \mathbf{1} \otimes \mathcal{A}_m^{\text{full}} \otimes \mathcal{A}_e^{\text{full}}$, we only need to note that operators X_1, X_2, Z_1, Z_2 span the whole algebra $\mathcal{Q}_1 \otimes \mathcal{Q}_2$. \square

Proof of Lemma 12. We first recall that we order the plaquette observables $\{\mathbf{Z}_p\}_p$ as $\{\mathbf{Z}_j\}_{j=1}^{L^2}$ and index $\{\sigma_j^x\}_{j=2}^{L^2}$ along the snake. We note from (4.14) that the projections, as elements in $\mathcal{A}_m^{\text{full}}$, can be represented as

$$P_j^0 = (|+-\rangle\langle +-| + |-+\rangle\langle -+|)_{j-1,j}, \quad P_j^\pm = (|\mp\rangle\langle \mp|)_{j-1,j},$$

where the subscript means that the operator only nontrivially acts on bonds $j-1$ and j on the snake associated with observables $\{\mathbf{Z}_p\}_p$. This enables us to compute the jumps

³More rigorously, $|m\rangle = \sigma_{j_1}^x \cdots \sigma_{j_k}^x | +1^{L^2} \rangle$ is defined as the bond configuration for $\{\mathbf{Z}_p\}_p$ associated with the spin configuration $\sigma_{j_1}^x \cdots \sigma_{j_k}^x |\psi_o\rangle$, where $|\psi_o\rangle$ is a ground state (4.5).

$a_j, a_j^\dagger, a_j^0 \in \mathcal{A}_m^{\text{full}}$ defined in (4.15) for the local Lindbladian \mathcal{L}_1 in (4.32):

$$a_j = (|++\rangle \langle --|)_{j-1,j}, \quad a_j^\dagger = (|--\rangle \langle ++|)_{j-1,j},$$

and

$$a_j^0 = (|+-\rangle \langle -+| + |-+\rangle \langle +-|)_{j-1,j}.$$

Without loss of generality, we consider the Lindbladian $\mathcal{L}_{\sigma_j^x}$ in (4.16) for a fixed $j \in \Gamma_{\text{flip}}, \Gamma_{\text{ab}}, \Gamma_{\text{int}}$ on $\mathcal{A}_m^{\text{full}}(\Lambda)$ for each Λ . Due to the locality of the jump operators, $\mathcal{L}_{\sigma_j^x}$ only changes the pair of bonds associated with j . For simplicity, we shall omit the subscripts $j-1, j$.

- For $j \in \Gamma_{\text{ab}}$, we consider the local basis

$$A_1 = |++\rangle \langle ++|, \quad A_2 = |+-\rangle \langle +-|, \quad A_3 = |-+\rangle \langle -+|, \quad A_4 = |--\rangle \langle --|,$$

that are orthogonal in both HS and GNS inner products for the reduced Gibbs state $\tilde{\sigma}_\beta = \text{Tr}_{\mathcal{A}_e^{\text{full}}}(\sigma_\beta) \propto \exp(-\beta \sum_p \mathbf{Z}_p)$. Moreover, we compute

$$\begin{aligned} e^{-\beta \sum_p \mathbf{Z}_p} A_1 &= \eta^{-1} A_1, & e^{-\beta \sum_p \mathbf{Z}_p} A_2 &= A_2, \\ e^{-\beta \sum_p \mathbf{Z}_p} A_3 &= A_3, & e^{-\beta \sum_p \mathbf{Z}_p} A_4 &= \eta A_4, \end{aligned}$$

where $\eta = e^{-2\beta}$, which implies that

$$\|A_1\|_{\tilde{\sigma}_\beta} = \mathcal{Z}_\beta^{-1/2} \eta^{-1/2}, \quad \|A_2\|_{\tilde{\sigma}_\beta} = \|A_3\|_{\tilde{\sigma}_\beta} = \mathcal{Z}_\beta^{-1/2}, \quad \|A_4\|_{\tilde{\sigma}_\beta} = \mathcal{Z}_\beta^{-1/2} \eta^{1/2},$$

with \mathcal{Z}_β being the partition function of σ_β . Then, we find, by using (4.16),

$$\mathcal{L}_{\sigma_j^x}(A_1) = h_+ |--\rangle \langle --| - h_- |++\rangle \langle ++| = h_+ A_4 - h_- A_1$$

due to

$$\begin{aligned} [A_1, a_j] &= [|++\rangle \langle ++|, |++\rangle \langle --|] = |++\rangle \langle --|, \\ [A_1, a_j^\dagger] &= [|++\rangle \langle ++|, |--\rangle \langle ++|] = -|--\rangle \langle ++|. \end{aligned}$$

Similarly, we have $\mathcal{L}_{\sigma_j^x}(A_4) = -h_+ A_4 + h_- A_1$, by

$$\begin{aligned} [A_4, a_j] &= [|--\rangle \langle --|, |++\rangle \langle --|] = -|++\rangle \langle --|, \\ [A_4, a_j^\dagger] &= [|--\rangle \langle --|, |--\rangle \langle ++|] = |--\rangle \langle ++|. \end{aligned}$$

In the same way, we can also compute

$$\mathcal{L}_{\sigma_j^x}(A_2) = A_3 - A_2, \quad \mathcal{L}_{\sigma_j^x}(A_3) = A_2 - A_3.$$

This allows us to compute the local matrix representation of the master Hamiltonian

$\varphi \circ \mathcal{L}_1 \circ \varphi^{-1}$ via $\frac{\langle A_i, \mathcal{L}_1 A_j \rangle_{\tilde{\sigma}_\beta}}{\|A_i\|_{\tilde{\sigma}_\beta} \|A_j\|_{\tilde{\sigma}_\beta}}$:

$$\begin{bmatrix} -h_- = -\frac{2\eta^2}{\eta^2+1} & 0 & 0 & h_-/\eta = \frac{2\eta}{\eta^2+1} \\ 0 & -1 & 1 & 0 \\ 0 & 1 & -1 & 0 \\ \eta h_+ = \frac{2\eta}{\eta^2+1} & 0 & 0 & -h_+ = -\frac{2}{\eta^2+1} \end{bmatrix}. \quad (4.52)$$

- For $j \in \Gamma_{\text{flip}}$, we let

$$A_1 = |++\rangle \langle --|, \quad A_2 = |+-\rangle \langle -+|, \quad A_3 = |-+\rangle \langle +-|, \quad A_4 = |--\rangle \langle ++|.$$

For A_1, A_4 , noting that

$$\begin{aligned} [A_1, a_j] &= [|++\rangle \langle --|, |++\rangle \langle --|] = 0, \\ [A_1, a_j^\dagger] &= [|++\rangle \langle --|, |--\rangle \langle ++|] = |++\rangle \langle ++| - |--\rangle \langle --|, \end{aligned}$$

and

$$\begin{aligned} [A_4, a_j] &= [|--\rangle \langle ++|, |++\rangle \langle --|] = |--\rangle \langle --| - |++\rangle \langle ++|, \\ [A_4, a_j^\dagger] &= [|--\rangle \langle ++|, |--\rangle \langle ++|] = 0, \end{aligned}$$

we have

$$\mathcal{L}_{\sigma_j^x}(A_1) = \frac{1}{2} \left\{ h_+[a_j^\dagger, A_1]a_j + h_-a_j[A_1, a_j^\dagger] \right\} = -\frac{1}{2}(h_+ + h_-)A_1,$$

and

$$\mathcal{L}_{\sigma_j^x}(A_4) = \frac{1}{2} \left\{ h_+a_j^\dagger[A_4, a_j] + h_-[a_j, A_4]a_j^\dagger \right\} = -\frac{1}{2}(h_+ + h_-)A_4.$$

Similarly, a direct computation also gives

$$\mathcal{L}_{\sigma_j^x}(A_2) = A_3 - A_2, \quad \mathcal{L}_{\sigma_j^x}(A_3) = A_2 - A_3.$$

The local matrix representation of $\varphi \circ \mathcal{L}_1 \circ \varphi^{-1}$ via $\frac{\langle A_i, \mathcal{L}_1 A_j \rangle_{\bar{\sigma}_\beta}}{\|A_i\|_{\bar{\sigma}_\beta} \|A_j\|_{\bar{\sigma}_\beta}}$ is given by

$$\begin{bmatrix} -\frac{h_++h_-}{2} & 0 & 0 & 0 \\ 0 & -1 & 1 & 0 \\ 0 & 1 & -1 & 0 \\ 0 & 0 & 0 & -\frac{h_++h_-}{2} \end{bmatrix}. \quad (4.53)$$

- For $j \in \Gamma_{\text{int}}$, we let⁴

$$A_1 = |++\rangle \langle -+|, \quad A_2 = |+-\rangle \langle --|, \quad A_3 = |-+\rangle \langle ++|, \quad A_4 = |--\rangle \langle +-|.$$

and find that they are eigenvectors of $\mathcal{L}_{\sigma_j^x}$:

$$\mathcal{L}_{\sigma_j^x}(A_1) = -\frac{h_- + 1}{2}A_1, \quad \mathcal{L}_{\sigma_j^x}(A_2) = -\frac{h_+ + 1}{2}A_2,$$

and

$$\mathcal{L}_{\sigma_j^x}(A_3) = -\frac{h_- + 1}{2}A_3, \quad \mathcal{L}_{\sigma_j^x}(A_4) = -\frac{h_+ + 1}{2}A_4.$$

⁴Without loss of generality, we place $j \in \Lambda$ in the second position. The other case of $j-1 \in \Lambda$ is symmetric.

In this case, the local matrix representation of $\varphi \circ \mathcal{L}_1 \circ \varphi^{-1}$ via $\frac{\langle A_i, \mathcal{L}_1 A_j \rangle_{\tilde{\sigma}_\beta}}{\|A_i\|_{\tilde{\sigma}_\beta} \|A_j\|_{\tilde{\sigma}_\beta}}$ is

$$\begin{bmatrix} -\frac{h_-+1}{2} & 0 & 0 & 0 \\ 0 & -\frac{h_++1}{2} & 0 & 0 \\ 0 & 0 & -\frac{h_-+1}{2} & 0 \\ 0 & 0 & 0 & -\frac{h_++1}{2} \end{bmatrix}. \quad (4.54)$$

The above calculation concludes the proof that \mathcal{L}_1 is block diagonal for the decomposition of $\mathcal{A}_m^{\text{full}}$ in (4.34), namely, $\mathcal{L}_1 : \mathcal{B}(\mathcal{H}_+)(\Lambda) \rightarrow \mathcal{B}(\mathcal{H}_+)(\Lambda)$ for any $\Lambda \subset \{1, 2, \dots, L^2\}$ such that $L^2 - |\Lambda|$ is even. \square

References

- [ACL23] Dong An, Andrew M Childs, and Lin Lin. Quantum algorithm for linear non-unitary dynamics with near-optimal dependence on all parameters. *arXiv preprint arXiv:2312.03916*, 2023.
- [AFH09] R Alicki, M Fannes, and M Horodecki. On thermalization in kitaev’s 2d model. *Journal of Physics A: Mathematical and Theoretical*, 42(6):065303, January 2009.
- [AHHH10] R. Alicki, M. Horodecki, P. Horodecki, and R. Horodecki. On thermal stability of topological qubit in kitaev’s 4d model. *Open Systems and Information Dynamics*, 17(01):1–20, 2010.
- [Bar82] Francisco Barahona. On the computational complexity of ising spin glass models. *Journal of Physics A: Mathematical and General*, 15(10):3241, 1982.
- [BCG⁺23] Ivan Bardet, Ángela Capel, Li Gao, Angelo Lucia, David Pérez-García, and Cambyse Rouzé. Rapid thermalization of spin chain commuting Hamiltonians. *Phys. Rev. Lett.*, 130(6):060401, 2023.
- [BCG⁺24] Ivan Bardet, Ángela Capel, Li Gao, Angelo Lucia, David Pérez-García, and Cambyse Rouzé. Entropy decay for davies semigroups of a one dimensional quantum lattice. *Communications in Mathematical Physics*, 405(2):42, 2024.
- [BCGW21] Sergey Bravyi, Anirban Chowdhury, David Gosset, and Pawel Wocjan. On the complexity of quantum partition functions. *arXiv preprint arXiv:2110.15466*, 2021.
- [BCL24] Thiago Bergamaschi, Chi-Fang Chen, and Yunchao Liu. Quantum computational advantage with constant-temperature gibbs sampling. *arXiv preprint arXiv:2404.14639*, 2024.
- [BCP⁺21] Antonio Blanca, Pietro Caputo, Daniel Parisi, Alistair Sinclair, and Eric Vigoda. Entropy decay in the swendsen–wang dynamics on \mathbb{Z}^d . In *Proceedings of the 53rd Annual ACM SIGACT Symposium on Theory of Computing*, pages 1551–1564, 2021.

- [BLMT24] Ainesh Bakshi, Allen Liu, Ankur Moitra, and Ewin Tang. High-Temperature Gibbs States are Unentangled and Efficiently Preparable. *arXiv preprint arXiv:2403.16850*, 2024.
- [BLP⁺16] Benjamin J. Brown, Daniel Loss, Jiannis K. Pachos, Chris N. Self, and James R. Wootton. Quantum memories at finite temperature. *Rev. Mod. Phys.*, 88:045005, Nov 2016.
- [Bom13] Héctor Bombín. An introduction to topological quantum codes. *arXiv preprint arXiv:1311.0277*, 2013.
- [BW00] Jeff P Barnes and Warren S Warren. Automatic quantum error correction. *Phys. Rev. Lett.*, 85(4):856, 2000.
- [CB21] Chi-Fang Chen and Fernando G.S.L. Brandão. Fast Thermalization from the Eigenstate Thermalization Hypothesis. *arXiv preprint arXiv:2112.07646*, 2021.
- [CGG⁺21] Zongchen Chen, Andreas Galanis, Leslie A Goldberg, Will Perkins, James Stewart, and Eric Vigoda. Fast algorithms at low temperatures via markov chains. *Random Structures & Algorithms*, 58(2):294–321, 2021.
- [CKBG23] Chi-Fang Chen, Michael J Kastoryano, Fernando GSL Brandão, and András Gilyén. Quantum thermal state preparation. *arXiv preprint arXiv:2303.18224*, 2023.
- [CKG23] Chi-Fang Chen, Michael J Kastoryano, and András Gilyén. An efficient and exact noncommutative quantum gibbs sampler. *arXiv preprint arXiv:2311.09207*, 2023.
- [CS17] Anirban Narayan Chowdhury and Rolando D. Somma. Quantum algorithms for Gibbs sampling and hitting-time estimation. *Quantum Inf. Comput.*, 17(1-2):41–64, 2017.
- [Dav70] EB Davies. Quantum stochastic processes ii. *Commun. Math. Phys.*, 19(2):83–105, 1970.
- [Dav74] E. Brian Davies. Markovian master equations. *Commun. Math. Phys.*, 39:91–110, 1974.
- [DLL24] Zhiyan Ding, Bowen Li, and Lin Lin. Efficient quantum gibbs samplers with Kubo–Martin–Schwinger detailed balance condition. *arXiv/2404.05998*, 2024.
- [FHGW14] C. Daniel Freeman, C. M. Herdman, D. J. Gorman, and K. B. Whaley. Relaxation dynamics of the toric code in contact with a thermal reservoir: Finite-size scaling in a low-temperature regime. *Phys. Rev. B*, 90:134302, Oct 2014.
- [Fre18] Christian Daniel Freeman. *The Toric Code at Finite Temperature*. PhD thesis, UC Berkeley, 2018.

- [GJ17] Heng Guo and Mark Jerrum. Random cluster dynamics for the ising model is rapidly mixing. In *Proceedings of the Twenty-Eighth Annual ACM-SIAM Symposium on Discrete Algorithms*, pages 1818–1827. SIAM, 2017.
- [GS22] Reza Gheissari and Alistair Sinclair. Low-temperature ising dynamics with random initializations. In *Proceedings of the 54th Annual ACM SIGACT Symposium on Theory of Computing*, pages 1445–1458, 2022.
- [GSLW19] András Gilyén, Yuan Su, Guang Hao Low, and Nathan Wiebe. Quantum singular value transformation and beyond: exponential improvements for quantum matrix arithmetics. In *Proceedings of the 51st Annual ACM SIGACT Symposium on Theory of Computing*, pages 193–204, 2019.
- [GŠV19] Andreas Galanis, Daniel Štefankovič, and Eric Vigoda. Swendsen-wang algorithm on the mean-field potts model. *Random Structures & Algorithms*, 54(1):82–147, 2019.
- [HPR19] Tyler Helmuth, Will Perkins, and Guus Regts. Algorithmic pirogov-sinai theory. In *Proceedings of the 51st Annual ACM SIGACT Symposium on Theory of Computing*, pages 1009–1020, 2019.
- [JS93] Mark Jerrum and Alistair Sinclair. Polynomial-time approximation algorithms for the ising model. *SIAM Journal on computing*, 22(5):1087–1116, 1993.
- [KACR24] Jan Kochanowski, Alvaro M. Alhambra, Angela Capel, and Cambyse Rouzé. Rapid thermalization of dissipative many-body dynamics of commuting hamiltonians. *arXiv/2404.16780*, 2024.
- [KB16] Michael J. Kastoryano and Fernando G.S.L. Brandão. Quantum Gibbs samplers: The commuting case. *Commun. Math. Phys.*, 344:915–957, 2016.
- [KFGV77] Andrzej Kossakowski, Alberto Frigerio, Vittorio Gorini, and Maurizio Verri. Quantum detailed balance and KMS condition. *Commun. Math. Phys.*, 57(2):97–110, 1977.
- [Kit03] A Yu Kitaev. Fault-tolerant quantum computation by anyons. *Annals of physics*, 303(1):2–30, 2003.
- [KKCG24] Michael J. Kastoryano, Lasse B. Kristensen, Chi-Fang Chen, and András Gilyén. A little bit of self-correction. *arXiv/2408.14970*, 2024.
- [KN97] Tohru Koma and Bruno Nachtergaele. The spectral gap of the ferromagnetic XXZ-chain. *Letters in Mathematical Physics*, 40:1–16, 1997.
- [KT13] Michael J Kastoryano and Kristan Temme. Quantum logarithmic Sobolev inequalities and rapid mixing. *J. Math. Phys.*, 54(5):1–34, 2013.
- [LKV⁺13] Zaki Leghtas, Gerhard Kirchmair, Brian Vlastakis, Robert J Schoelkopf, Michel H Devoret, and Mazyar Mirrahimi. Hardware-efficient autonomous quantum memory protection. *Phys. Rev. Lett.*, 111(12):120501, 2013.

- [LLG24] Simon Lieu, Yu-Jie Liu, and Alexey V. Gorshkov. Candidate for a passively protected quantum memory in two dimensions. *Phys. Rev. Lett.*, 133:030601, Jul 2024.
- [LS16] Eyal Lubetzky and Allan Sly. Information percolation and cutoff for the stochastic ising model. *Journal of the American Mathematical Society*, 29(3):729–774, 2016.
- [MH21] Ryan L Mann and Tyler Helmuth. Efficient algorithms for approximating quantum partition functions. *Journal of Mathematical Physics*, 62(2), 2021.
- [ML20] Evgeny Mozgunov and Daniel Lidar. Completely positive master equation for arbitrary driving and small level spacing. *Quantum*, 4(1):1–62, 2020.
- [MO94] Fabio Martinelli and Enzo Olivieri. Approach to equilibrium of glauher dynamics in the one phase region: I. the attractive case. *Communications in Mathematical Physics*, 161(3):447–486, 1994.
- [Pis96] Agoston Pisztora. Surface order large deviations for ising, potts and percolation models. *Probability Theory and Related Fields*, 104:427–466, 1996.
- [PW09] David Poulin and Pawel Wocjan. Preparing ground states of quantum many-body systems on a quantum computer. *Phys. Rev. Lett.*, 102(13):130503, 2009.
- [RFA24] Cambyse Rouzé, Daniel Stilck Franca, and Álvaro M. Alhambra. Efficient thermalization and universal quantum computing with quantum Gibbs samplers. *arXiv preprint arXiv:2403.12691*, 2024.
- [RW24] Joel Rajakumar and James D Watson. Gibbs sampling gives quantum advantage at constant temperatures with $o(1)$ -local hamiltonians. *arXiv preprint arXiv:2408.01516*, 2024.
- [RWW23] Patrick Rall, Chunhao Wang, and Pawel Wocjan. Thermal state preparation via rounding promises. *Quantum*, 7:1132, 2023.
- [Sly10] Allan Sly. Computational transition at the uniqueness threshold. In *2010 IEEE 51st Annual Symposium on Foundations of Computer Science*, pages 287–296. IEEE, 2010.
- [Tem17] Kristan Temme. Thermalization time bounds for pauli stabilizer hamiltonians. *Communications in Mathematical Physics*, 350(2):603–637, 2017.
- [TK15] Kristan Temme and Michael J. Kastoryano. How fast do stabilizer hamiltonians thermalize? *arXiv/1505.07811*, 2015.
- [TKR⁺10] Kristan Temme, Michael James Kastoryano, Mary Beth Ruskai, Michael Marc Wolf, and Frank Verstraete. The χ^2 -divergence and mixing times of quantum Markov processes. *J. Math. Phys.*, 51(12), 2010.

- [VAGGdW17] Joran Van Apeldoorn, András Gilyén, Sander Gribling, and Ronald de Wolf. Quantum SDP-solvers: Better upper and lower bounds. In *FOCS 2017*, pages 403–414. IEEE, 2017.
- [VWC09] Frank Verstraete, Michael M. Wolf, and I. Cirac. Quantum computation and quantum-state engineering driven by dissipation. *Nat. Phys.*, 5(9):633–636, 2009.
- [Wol12] Michael M. Wolf. Quantum channels & operations: guided tour. Lecture Notes. URL [http://www-m5.ma.tum.de/foswiki/pub M](http://www-m5.ma.tum.de/foswiki/pub/M), 2012.
- [WT23] Pawel Wocjan and Kristan Temme. Szegedy walk unitaries for quantum maps. *Commun. Math. Phys.*, 402(3):3201–3231, 2023.
- [YL23] Chao Yin and Andrew Lucas. Polynomial-time classical sampling of high-temperature quantum gibbs states. *arXiv preprint arXiv:2305.18514*, 2023.
- [ZB23] Yikang Zhang and Thomas Barthel. Criteria for Davies irreducibility of Markovian quantum dynamics. *J. Phys. A: Math. Theor*, 2023.

A Low temperature Gibbs state preparation for 1D ferromagnetic Ising model

This section studies the low-temperature thermal state preparation for a 1D ferromagnetic Ising chain with periodic boundary condition. Although the Hamiltonian of this model is classical (a diagonal matrix in the computational basis), the jump operators are quantum and involve a significant amount of non-diagonal elements. The analysis of this model also shows the generality of core techniques for the 2D toric code in Section 4.

We consider N spins on a ring structure, modeled by the Hilbert space $\mathcal{H} \cong \mathbb{C}^{2^N}$. The Hamiltonian is

$$H^{\text{Ising}} = -J \sum_{j=1}^N \sigma_j^z \sigma_{j+1}^z, \quad J > 0, \quad (\text{A.1})$$

with $\sigma_{N+1}^z = \sigma_1^z$ (see Fig. 7, top), where $\{\mathbf{Z}_j := \sigma_j^z \sigma_{j+1}^z\}_{j=1}^N$ are bond observables satisfying

$$\prod_{j=1}^N \mathbf{Z}_j = I. \quad (\text{A.2})$$

We propose the following Gibbs smaller for the above Ising model:

$$\mathcal{L}_\beta = \sum_{j=1}^N \left(\mathcal{L}_{\sigma_j^x} + \mathcal{L}_{\sigma_j^y} + \mathcal{L}_{\sigma_j^z} \right) + \mathcal{L}_X, \quad (\text{A.3})$$

which is the sum of local Lindbladians with Pauli couplings plus a global one with coupling operator $X := \prod_{j=1}^N \sigma_j^x$. Here $\mathcal{L}_{\sigma_j^{x/y/z}}$ and \mathcal{L}_X are defined via (2.4). Their explicit formulas can be similarly derived as in (4.16), (4.18), and (4.19). The main result of this section is the following spectral gap lower bound of \mathcal{L}_β in Eq. (A.3).

Theorem 17. For the Davies generator (A.3), we have

$$\text{Gap}(\mathcal{L}_\beta) \geq \max \left\{ \Theta(e^{-4\beta J}), \Theta(N^{-3}) \right\}.$$

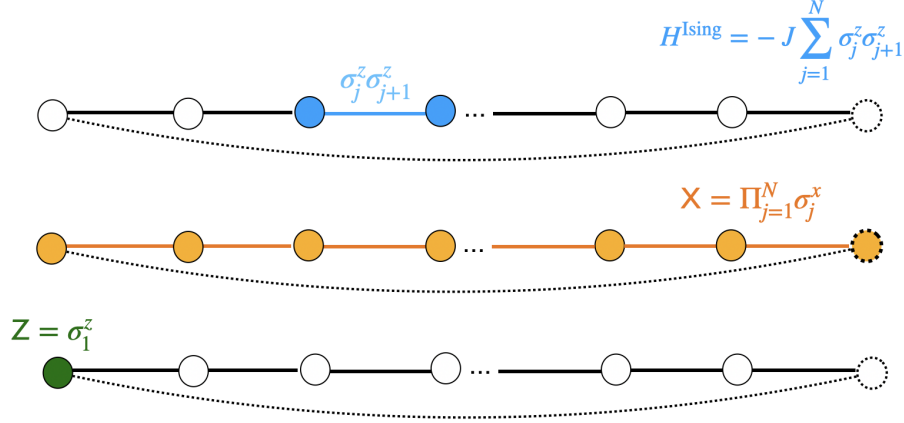


Figure 7: 1D Ising model. *Top*: The 1D ferromagnetic Ising Hamiltonian H^{Ising} . The dashed dot and line denote the periodic boundary condition. *Middle*: The logic operator $X = \prod_{i=1}^N \sigma_i^x$. *Bottom*: The logic operator $Z = \sigma_1^z$.

The proof is similar to that of Theorem 1, based on the structures of the ground states of the Ising model and the associated observable algebra $\mathcal{B}(\mathcal{H})$. We know that H^{Ising} has a two-fold degenerate ground state space spanned by $|0^N\rangle$ and $|1^N\rangle$, and it is frustration-free, namely, any ground state $|\varphi\rangle$ of H^{Ising} satisfies $\sigma_j^z \sigma_{j+1}^z |\varphi\rangle = |\varphi\rangle$ for each j . This two two-fold degeneracy encodes a single logical qubit in the sense that with some abuse of notation, $|0^N\rangle$ and $|1^N\rangle$ can be identified as the logical qubit $|0\rangle$ and as $|1\rangle$, respectively:

$$|0\rangle \simeq |0^N\rangle, \quad |1\rangle \simeq |1^N\rangle.$$

The excited states are given by acting Pauli string $X_{j_1} \cdots X_{j_n}$ on the ground states $|0^N\rangle$ and $|1^N\rangle$. We define observables (see Fig. 7)

$$X = \prod_{i=1}^N \sigma_i^x, \quad Z = \sigma_1^z.$$

The observable X flips the logical qubit $X|0/1\rangle = |1/0\rangle$. The measurement outcome by Z indicates which state we are observing:

$$\langle 0|Z|0\rangle = 1, \quad \langle 1|Z|1\rangle = -1.$$

We note that X and Z commute with local terms $\{\sigma_j^z \sigma_{j+1}^z\}$, and thus all the eigenspaces of H^{Ising} are the invariant subspaces of X and Z .

Let $\mathcal{Q} \cong \mathcal{B}(\mathbb{C}^2)$ be the algebra on the logical qubit generated by X and Z . Then we have $\mathcal{Q} = \text{Span}\{I, X, Y, Z\}$, where $Y = iZX$. To describe the excited states and observable algebra

$\mathcal{B}(\mathcal{H})$, we first define an admissible bond on a ring of N sites as a configuration containing an even number of -1 :

$$|b\rangle = |b_1, b_2, \dots, b_N\rangle \in \{+1, -1\}^N \text{ such that } \#\{b_i = -1\} \in 2\mathbb{Z}.$$

The space spanned by the admissible bond, denoted by \mathcal{H}_+ , is of dimension 2^{N-1} . An important observation is that a natural orthonormal tensor basis of \mathbb{C}^{2^N} consisting of $|\epsilon_1 \dots \epsilon_N\rangle$ with $\epsilon_i = 0/1$ can be uniquely written as $|\epsilon_1\rangle |b\rangle \in \mathbb{C}^2 \otimes \mathcal{H}_+$, where the first qubit $|\epsilon_1\rangle$ is regarded as a logical qubit and b_j is determined by the bond observable $\mathbf{Z}_j = \sigma_j^z \sigma_{j+1}^z$:

$$\mathbf{Z}_j |\epsilon_1 \dots \epsilon_N\rangle = b_j |\epsilon_1 \dots \epsilon_N\rangle.$$

We define the full bond algebra $\mathcal{A}_b^{\text{full}}$ by all the linear transformations on \mathcal{H}_+ . Then, as a consequence of the above decomposition of $|\epsilon_1 \dots \epsilon_N\rangle$, the observable algebra can be decomposed as follows [AFH09, Lemma 4].

Lemma 18. *The algebra of observables on a ring can be decomposed into*

$$\mathcal{B}(\mathcal{H}) = \mathcal{Q} \otimes \mathcal{A}_b^{\text{full}}.$$

In particular, we have the orthogonal decomposition in GNS inner product

$$\mathcal{B}(\mathcal{H}) = (I \otimes \mathcal{A}_b^{\text{full}}) \oplus (\mathbf{X} \otimes \mathcal{A}_b^{\text{full}}) \oplus (\mathbf{Y} \otimes \mathcal{A}_b^{\text{full}}) \oplus (\mathbf{Z} \otimes \mathcal{A}_b^{\text{full}}). \quad (\text{A.4})$$

We are now ready to sketch the proof of Theorem 17. For simplicity, we use $b_j = \pm$ for the bond configuration. Similarly to Lemma 5, the algebra $\mathcal{A}_b^{\text{full}}$ is generated by the observables $\{\mathbf{Z}_j\}_{j=1}^N$ and $\{\sigma_j^x\}_{j=2}^N$, which commute with \mathbf{X} . Then, by a direct computation, we have $\mathcal{L}_{\mathbf{X}}(I \otimes \mathcal{A}_b^{\text{full}}) = 0$. Moreover, there holds

$$\mathcal{L}_{\mathbf{X}}(\mathbf{Z}/\mathbf{Y} \otimes \mathcal{A}_b^{\text{full}}) = -2(\mathbf{Z}/\mathbf{Y}) \otimes \mathcal{A}_b^{\text{full}}, \quad -\langle (\mathbf{Z}/\mathbf{Y}), \mathcal{L}_{\mathbf{X}}(\mathbf{Z}/\mathbf{Y}) \rangle_{\sigma_\beta} = 2. \quad (\text{A.5})$$

Similarly, we derive $\mathcal{L}_{\mathbf{Z}}(I \otimes \mathcal{A}_b^{\text{full}}) = 0$, and

$$\mathcal{L}_{\mathbf{Z}}(\mathbf{X}/\mathbf{Y} \otimes \mathcal{A}_b^{\text{full}}) = -2(\mathbf{X}/\mathbf{Y}) \otimes \mathcal{A}_b^{\text{full}}, \quad -\langle (\mathbf{X}/\mathbf{Y}), \mathcal{L}_{\mathbf{Z}}(\mathbf{X}/\mathbf{Y}) \rangle_{\sigma_\beta} = 2. \quad (\text{A.6})$$

Further, for the action of local Lindbladian $\mathcal{L}_{\sigma_j^x/\sigma_j^y/\sigma_j^z}$ on the decomposition (A.4), we have the following lemma, in analog with Lemma 6.

Lemma 19. *The Lindbladian with Pauli coupling $\mathcal{L}_{\sigma_j^x}$, $\mathcal{L}_{\sigma_j^y}$, and $\mathcal{L}_{\sigma_j^z}$ ($j \geq 1$) are block diagonal with respect to the decomposition (A.4):*

$$\mathcal{L}_{\sigma_j^x/\sigma_j^y/\sigma_j^z}(I/\mathbf{X}/\mathbf{Y}/\mathbf{Z} \otimes \mathcal{A}_b^{\text{full}}) \subset I/\mathbf{X}/\mathbf{Y}/\mathbf{Z} \otimes \mathcal{A}_b^{\text{full}}.$$

In particular, it holds that for $j \geq 2$, $\mathcal{L}_{\sigma_j^x}(\mathcal{Q} \otimes \mathcal{A}_b^{\text{full}}) = \mathcal{Q} \otimes \mathcal{L}_{\sigma_j^x}(\mathcal{A}_b^{\text{full}})$, that is,

$$\mathcal{L}_{\sigma_j^x}(QA) = Q\mathcal{L}_{\sigma_j^x}(A) \quad \text{for } Q \in \mathcal{Q} \text{ and } A \in \mathcal{A}_b^{\text{full}}.$$

We now define the local Lindbladian:

$$\tilde{\mathcal{L}} = \sum_{j=2}^N \mathcal{L}_{\sigma_j^x} \quad (\text{A.7})$$

which is primitive when restricted on $\mathcal{B}(\mathcal{H}_+) = \mathcal{A}_b^{\text{full}}$ [AFH09, Lemma 6]. Thanks to the properties (A.5)–(A.6) of \mathcal{L}_X and \mathcal{L}_Z , the Lindbladian $\tilde{\mathcal{L}} + \mathcal{L}_X + \mathcal{L}_Z$ (as a part of \mathcal{L}_β in (A.3)) is primitive on $\mathcal{B}(\mathcal{H})$. Then, Lemma 3 (item 2) readily gives

$$\text{Gap}(\mathcal{L}_\beta) \geq \text{Gap}\left(\tilde{\mathcal{L}} + \mathcal{L}_X + \mathcal{L}_Z\right). \quad (\text{A.8})$$

Thus, it suffices to consider the spectral gap of the latter one. For this, we note from (A.5)–(A.6) that $\mathcal{L}_{X/Z}$ is also block diagonal for the decomposition (A.4). Then, by Lemma 19, we only need to estimate the gap of $\tilde{\mathcal{L}} + \mathcal{L}_X + \mathcal{L}_Z$ on each invariant subspace $I/X/Y/Z \otimes \mathcal{A}_b^{\text{full}}$:

- On $I \otimes \mathcal{A}_b^{\text{full}}$. Noting $\mathcal{L}_X|_{I \otimes \mathcal{A}_b^{\text{full}}} = \mathcal{L}_Z|_{I \otimes \mathcal{A}_b^{\text{full}}} = 0$, we have

$$\text{Gap}\left(\left(\tilde{\mathcal{L}} + \mathcal{L}_X + \mathcal{L}_Z\right)\Big|_{I \otimes \mathcal{A}_b^{\text{full}}}\right) = \text{Gap}\left(\tilde{\mathcal{L}}\Big|_{I \otimes \mathcal{A}_b^{\text{full}}}\right).$$

- On $X/Y/Z \otimes \mathcal{A}_b^{\text{full}}$. Noting that any Davies generator is negative, we have

$$-\left(\tilde{\mathcal{L}} + \mathcal{L}_X + \mathcal{L}_Z\right)\Big|_{Z \otimes \mathcal{A}_b^{\text{full}}} \succeq -\left(\tilde{\mathcal{L}} + \mathcal{L}_X\right)\Big|_{Z \otimes \mathcal{A}_b^{\text{full}}}.$$

Moreover, $\ker\left(\tilde{\mathcal{L}}\Big|_{Z \otimes \mathcal{A}_b^{\text{full}}}\right) = \text{Span}(Z \otimes I)$. It can be seen as follows. For any $ZA \in Z \otimes \mathcal{A}_b^{\text{full}}$ in the kernel, by the second part of Lemma 19, $\tilde{\mathcal{L}}(ZA) = Z\tilde{\mathcal{L}}(A) = 0$. Thus, $A \in \ker\left(\tilde{\mathcal{L}}\Big|_{\mathcal{A}_b^{\text{full}}}\right)$. Since $\tilde{\mathcal{L}}\Big|_{\mathcal{A}_b^{\text{full}}}$ is primitive, it must be the case that $A = I$. Then, by Lemma 3 (item 4), there holds

$$-\left(\tilde{\mathcal{L}} + \mathcal{L}_X\right)\Big|_{Z \otimes \mathcal{A}_b^{\text{full}}} \succeq \frac{-\text{Gap}\left(\tilde{\mathcal{L}}\Big|_{I \otimes \mathcal{A}_b^{\text{full}}}\right) \langle Z, \mathcal{L}_X(Z) \rangle_{\sigma_\beta}}{\text{Gap}\left(\tilde{\mathcal{L}}\Big|_{I \otimes \mathcal{A}_b^{\text{full}}}\right) + \|\mathcal{L}_X\|} = \Theta\left(\frac{\text{Gap}\left(\tilde{\mathcal{L}}\Big|_{I \otimes \mathcal{A}_b^{\text{full}}}\right)}{\text{Gap}\left(\tilde{\mathcal{L}}\Big|_{I \otimes \mathcal{A}_b^{\text{full}}}\right) + 1}\right).$$

The same estimates hold for $-\left(\tilde{\mathcal{L}} + \mathcal{L}_X\right)\Big|_{Y \otimes \mathcal{A}_b^{\text{full}}}$ and $-\left(\tilde{\mathcal{L}} + \mathcal{L}_Z\right)\Big|_{X \otimes \mathcal{A}_b^{\text{full}}}$.

Combining the above arguments with (A.8), we find

$$\begin{aligned} \text{Gap}(\mathcal{L}_\beta) &\geq \min\left\{\text{Gap}\left(-\left(\tilde{\mathcal{L}} + \mathcal{L}_X + \mathcal{L}_Z\right)\Big|_{I \otimes \mathcal{A}_b^{\text{full}}}\right), \lambda_{\min}\left(-\left(\tilde{\mathcal{L}} + \mathcal{L}_X + \mathcal{L}_Z\right)\Big|_{X/Y/Z \otimes \mathcal{A}_b^{\text{full}}}\right)\right\} \\ &= \Theta\left(\text{Gap}\left(\tilde{\mathcal{L}}\Big|_{I \otimes \mathcal{A}_b^{\text{full}}}\right)\right), \end{aligned}$$

as $\text{Gap}\left(\tilde{\mathcal{L}}\Big|_{I \otimes \mathcal{A}_b^{\text{full}}}\right) \rightarrow 0$. It has been proved in [AFH09, Proposition 1] that for any N ,

$$\text{Gap}\left(\tilde{\mathcal{L}}\Big|_{I \otimes \mathcal{A}_b^{\text{full}}}\right) \geq \frac{e^{-4\beta J}}{e^{-4\beta J} + 1}.$$

Therefore, to prove Theorem 17, it suffices to focus on the gap of $\tilde{\mathcal{L}}$ on $\mathcal{A}_b^{\text{full}}$ and show

$$\text{Gap}\left(\tilde{\mathcal{L}}\Big|_{I \otimes \mathcal{A}_b^{\text{full}}}\right) = \Omega(N^{-3}), \quad \text{when } \beta \geq \Omega(\log N), \quad (\text{A.9})$$

which can be done as Lemma 13. We have completed the proof of Theorem 17.